Chapter 5

Speedy Techniques to Evaluate Seismic Site Effects in Particular Geomorphologic Conditions: Faults, Cavities, Landslides and Topographic Irregularities

F. Panzera, G. Lombardo, S. D'Amico and P. Galea

Additional information is available at the end of the chapter

http://dx.doi.org/10.5772/55439

1. Introduction

The ground motion that can be recorded at the free surface of a terrain is the final result of a series of phenomena that can be grouped into three fundamental typologies: the source mechanism, the seismic wave propagation till the bedrock interface below the investigated site and the site effects (Fig. 1). The first two features define the kind of seismic input whereas the third represents all modifications that can occur as a consequence of the interaction between seismic waves and local characteristics of the investigated site. The physical and mechanical properties of terrains as well as their morphologic and stratigraphic features appreciably affect the characteristics of the ground motion observed at the surface. The whole process of modifications undergone by a given seismic input in terms of amplitude, frequency content and duration, as a consequence of local characteristics, is generally termed the "local seismic response". It is indeed well known that the spectral composition of a seismic event is modified first during the source-bedrock path (attenuation function), and second, when the seismic input interacts with the soft terrains layered between the bedrock and the free surface (Fig. 1a). This latter effect, significantly changes the spectral content so that it is extremely important for estimating the final input to which all structures built in the study area will be subjected.

The influence of local geologic features on the ground motion peculiarities and damage due to earthquakes is well known since years. Studies of Wood (1908) and Baratta (1910) concerning the San Francisco 1906 and the Messina 1908 earthquakes, respectively, pointed out, since the beginning of the last century, that the damage distribution is a function of different site conditions existing in various areas affected by the same shock. Similar effects have been observed by several authors during all destructive earthquakes occurred up till the present.

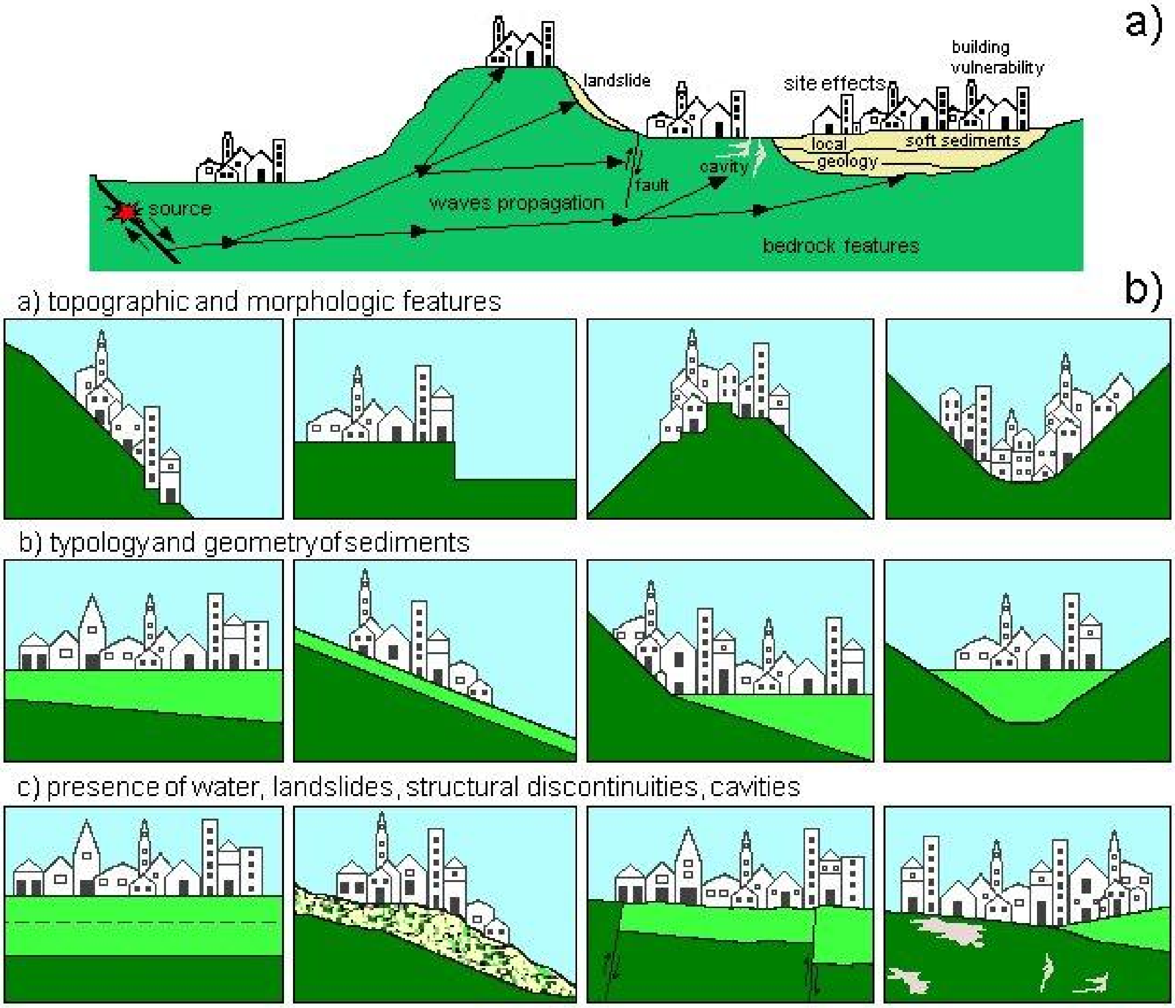

Figure 1. a) Sketch showing the influences that can affect a seismic signal propagating from the source to the free surface of a terrain. b) Scenaria for local seismic response.

Site effects occur as a result of several physical phenomena such as multiple reflections, diffraction, focusing, resonance etc., to which the incoming wavefront is subjected. This is a consequence of the various mechanical properties of terrains, the presence of heterogeneities and discontinuities, as well as the geometry of shallower layers and the existence of topographic irregularities both in the basement and the surface. In Figure 1b are shown the principal morphologic and/or structural features that contribute to characterize the local hazard scenario. They are grouped in effects linked to the layers' geometry (a), effects linked to the possible presence of water-bearing strata, landslides, structural discontinuities and cavities (b) and effects linked to the topography (c).

Generally stratigraphic effects are schematized as the modifications affecting a seismic motion that propagates almost vertically inside a deposit having a flat free surface, horizontal layers and negligible lateral heterogeneities. The theoretical analysis of such problem was tackled by Kramer (1996), and however, considering the described simplified assumptions, it can be postulated that the incident waves at the base of the deposit that are reflected at its free surface, are partially reflected again at the deposit-basement interface. The amount of reflected energy that is “trapped” into the deposit increases with the seismic impedance contrast between the terrains forming the deposit and the basement. Besides, the trapped waves interfere between themselves and the incident waves as a consequence of the geometric features of the deposit, the physical properties of the terrains and the frequency content of the seismic input. Stratigraphic site effects are therefore mainly connected to seismic wave trapping phenomena inside the deposit due to reflections as well as interference and resonance effects between incident and reflected waves. The local seismic response, becomes, of course, more complex when the basement-deposit interface has a more irregular geometry, or in the presence of faults, cavities and particular topographic conditions.

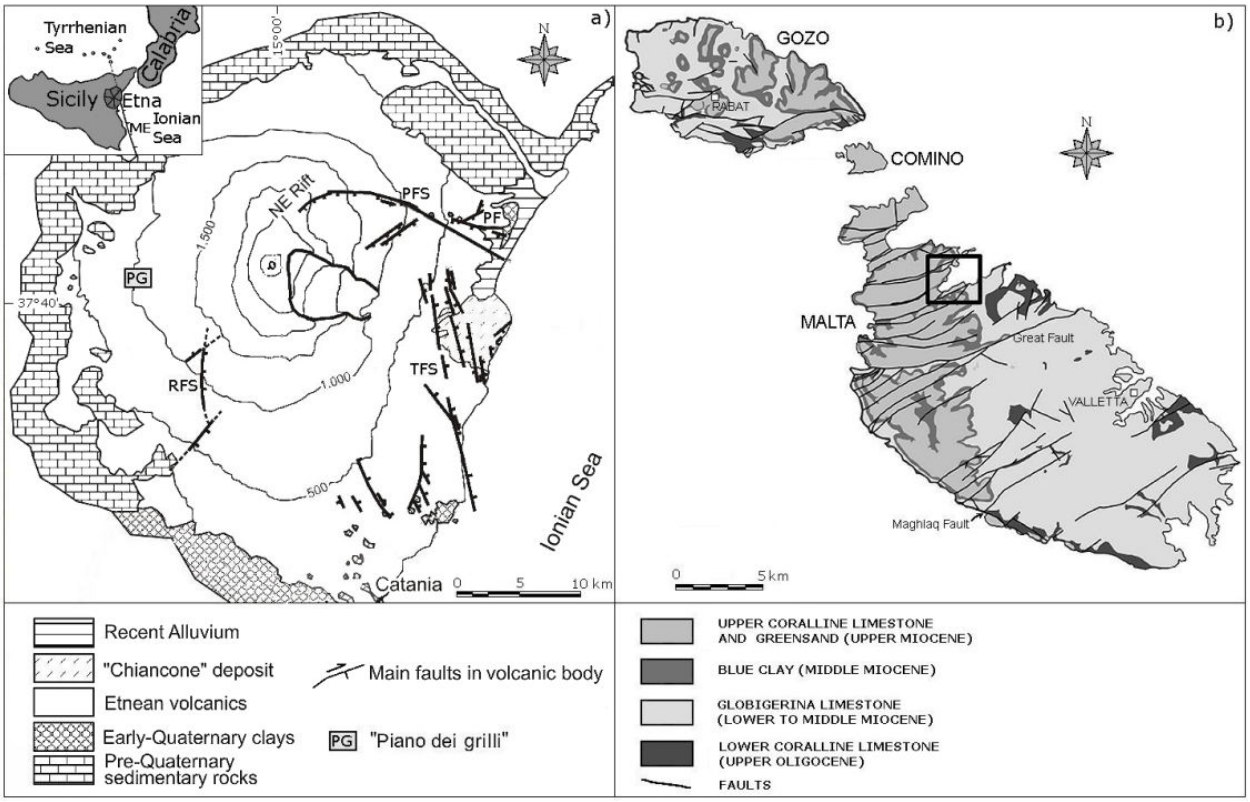

Figure 2. a) Simplified geological map of Mt Etna showing the main structural features (modified from Neri *et al.*, 2007), RFS = Ragalna fault system, PFS = Pernicana fault system, PF = Piedimonte fault, TFS = Timpe fault system. In the inset map, the Malta Escarpment (ME) is shown. (b) Sketch geological map of the Maltese Islands (modified from Various Authors, 1993). The black square indicates the investigated area.

In this study the characteristics of the local seismic response, linked in particular to the presence of discontinuities such as faults and cavities, as well as topographic irregularities and landslide phenomena, are investigated. Case-studies of sites located both in South-eastern Sicily and in Malta are described, illustrating, besides local amplification phenomena, the possible presence of directional effects.

2. Methodologies

Several different methodological approaches are commonly adopted to quantitatively assess the local seismic response. In practice, it is evaluated with respect to a reference site represented by the outcrop of a rocky basement (either real or supposed) existing in the investigated area. In other words, the local ground motion is compared with the one relative to a reference bedrock outcrop.

The site response can be evaluated through various approaches, also collateral between themselves, each of them having specific advantages and/or drawbacks well known in literature (see Pitilakis, 2004). Main methodologies can be grouped into two categories: numerical methods and experimental methods.

Numerical methods are founded on the use of computer codes that simulate wave propagation through soft deposits, from the bedrock to the free surface. Such codes allow the modelling of the dynamic behaviour of a terrain by adopting linear, equivalent-linear or non- linear models (e.g. SHAKE, Schnabel *et al*, 1972; EERA, Bardet *et al*, 2000; DESDRA, Lee e Finn, 1978) that can be either mono or multi-dimensional (Hudson *et al*, 1994). These methods provide in output the time history of involved seismic parameters and require as input data a detailed knowledge of the site geometry, the geotechnical properties of terrains and the stress-strain relationships.

The experimental methods allow us to evaluate the local seismic response using the records of seismic signals that be generated by earthquakes, artificial seismic sources or ambient noise. They are only moderately expensive and take implicitly into account all site effects, although their drawback is linked to the use of low or very low energy events, so that the seismic response evaluation is performed at low deformation levels and entirely in the linear field.

The results described in the present study, draw from the use of spectral ratios evaluated through comparison between the investigated site and the reference one (SSR *Standard Spectral Ratio* technique) and/or by calculating the spectral ratios between the horizontal and the vertical components of motion at the investigated site (HVSR *Horizontal to Vertical Spectral Ratio* and HVNR *Horizontal to Vertical Noise Ratio* or Nakamura method).

The SSR technique (Borcherdt 1970) consists in computing the Fourier spectral ratio of the same seismic waves (generally S waves) simultaneously recorded by the horizontal components of two seismic stations, one of which is located on a bedrock outcrop. The main difficulty associated with this technique is a proper choice of the reference site that has to be a flat outcrop of the bedrock. Moreover, the correct use of the SSR technique requires that the distance between test and reference sites has to be significantly smaller than the epicentral distance.

The earthquake HVSR, or receiver function technique, does not need a reference station and consists in the computation of the horizontal-to-vertical spectral ratio of the components of motion recorded at one seismic station only (Lermo and Chavez-Garcia 1993). This technique is founded on the assumption that the vertical component of motion is not affected by the local geological conditions. It is applied both to the time window of shear waves and to the entire seismic record and has shown to be a good approach for the evaluation of the site fundamental frequency whereas it appears less reliable for the estimate of the amplitude values.

The Nakamura technique (HVNR) (Nakamura, 1989) uses as a seismic input the ambient noise and computes the spectral ratio between the horizontal and the vertical components of motion. Ambient noise has, in recent years, become widely used for site amplification studies. Its use appears opportune for significant reductions in field data acquisition time and costs. The evaluation of site response using the HVNR technique is largely adopted since it requires only one mobile seismic station with no additional measurements at rock sites for comparison. Besides, it does not require the long and simultaneous deployment of several instruments which is necessary to collect a useful earthquake data set. The basic hypothesis of using ambient noise is that the resonance of a soft layer corresponds to the fundamental mode of Rayleigh waves, which is associated with an inversion of the direction of Rayleigh waves rotation (Nogoshi and Igarashi, 1970; Lachet and Bard, 1994). Thus, the ratio between the horizontal and vertical spectral components of motion can reveal the fundamental resonance frequency of the site. Reliability of such approach has been asserted by many authors (e.g. Lermo and Chavez-Garcıa, 1993; Bard, 1999) who have stressed its significant stability in local seismic response estimates. It is commonly accepted that, although the single components of ambient noise can show large spectral variations as a function of natural and cultural disturbances, the H/V spectral ratio tends to remain invariant, therefore preserving the fundamental frequency peak (Cara *et al*., 2003).

In the present study, ambient noise records were performed using a Tromino instrument (www.tromino.it), a compact 3-component velocimeter with a reliable instrumental response in the frequency range 0.5-10 Hz. The signals were processed by evaluating the horizontal-to-vertical noise spectral ratios (HVNR). Following the guidelines suggested by the European project Site EffectS assessment using AMbient Excitations (SESAME, 2004), time windows of 30 s were considered, selecting the most stationary part and excluding transients associated to very close sources. Fourier spectra were calculated and smoothed using a triangular average on frequency intervals of ± 5% of the central frequency.

The potential presence of directional effects in the ground motion recorded at the surface was also investigated. Such investigations can be done by computing the spectral ratios (SSR, HVSR, HVNR) after rotating the horizontal components by steps of 10° starting from 0° (north) to 180° (south) and plotting the contours of the spectral ratio amplitudes as a function of frequency and direction of motion. This approach (Spudich *et al*., 1996) is powerful in enhancing, if any, the occurrence of site specific directional effects. A direct estimate of the polarization angle, for noise data, can be achieved through two different methods. The time domain method (TD) by Jurkevics (1988) and the time-frequency (TF) polarization analysis by Burjánek *et al.* (2010 and 2012). The results obtained through polarization techniques are quite robust since these approaches are very efficient in overcoming the bias linked to the denominator behavior that could occur in the HVNR's technique and at the same time, longer time-series are processed therefore reducing the problems that may be linked to signal-to-noise ratio. In the TD approach, a direct estimate of the polarization angle is achieved by computing the polarization ellipsoid through the eigenvalues and eigenvectors of the covariance matrix obtained by three-component data (Jurkevics, 1988). The polarization ellipsoid of the analyzed signal is estimated by band-pass filtering it in the interval 1.0 - 10.0 Hz, using the whole recordings and considering a moving window of 1 s with 20% overlap, therefore obtaining the strike of maximum polarization for each moving time window. The results are finally plotted in circular histograms (rose diagrams) showing the polarization azimuths in intervals of ten degrees. In the TF method, a continuous wavelet transform for signal time-frequency decomposition, is firstly used. Subsequently, the polarization analysis on the complex wavelet amplitude for each time-frequency pair, is applied. In particular, histograms of the polarization parameters are created over time for each frequency. Polar plots are then adopted for depicting the final results, which illustrate the combined angular and frequency dependence.

3. Geologic and tectonic features of the studied areas

South-Eastern Sicily is located in a complex tectonic region being at the boundary between African and European plates (see inset map in Fig. 2a). Along this border, Mt. Etna, a basaltic volcano more than 3300 m high and with a diameter of about 40 km, resulting from the interaction of regional tectonics and local scale volcano-related processes (McGuire and Pullen, 1989), is sited. The island of Malta is placed in the Hyblean foreland, belonging to the African plate. Most of the formations here outcropping were deposited during the Oligocene and Miocene when the whole area was part of the Malta - Ragusa platform and, as such, attached to the African margin (Pedley *et al.*, 1978).

The whole study area is delineated by the crossing of lithosphere structures that give rise to the origin of Mt. Etna and by the presence of the Malta Hyblean fault system that runs down the Sicilian coast towards the Ionian sea (ME in the inset map of Fig. 2a). A series of horst and graben structures, NW-SE and NNW-SSE oriented, that are linked to the Malta-Hyblean escarpment, characterize indeed the tectonic setting of this area.

On Malta, the geo-structural pattern is dominated by two intersecting fault systems which alternate in tectonic activity. An older ENE-WSW trending fault, the Victoria Lines Fault (or Great Fault), traverses the islands and is crossed by a younger NW-SE trending fault, the Maghlaq Fault (Fig. 2b), parallel to the Malta trough which is the easternmost graben of the Pantelleria Rift system. The faults belonging to the older set, all vertical or sub vertical, are part of a horst and graben system of relatively small vertical displacement (Illies, 1981; Reuther et al. 1985).

As concerns Mt. Etna, its eastern flank is the more tectonically active part. Here, several NNW and NNE-trending fault segments (Timpe fault system, TFS), arranged in a 30 km long system (Fig. 2a), control the present topography and show steep escarpments with very sharp morphology (Monaco *et al.*, 1997). This system represents the northernmost prolongation of the Malta Escarpment and forms a system of parallel step-faults having vertical offsets up to 200 m that down-throw towards the sea. Most of these faults are highly seismogenic and generate shallow earthquakes as well as co-seismic cracks in the soil and creep phenomena (Azzaro, 1999). In the north eastern part of the area, the active Pernicana fault system (PFS) represent the most significant tectonic structure. It is a strike-slip fault roughly E-W oriented with a length of about 18 km from the NE rift to the coastline (Neri *et al*., 2004; Azzaro *et al*., 2001; Acocella and Neri, 2005). At the end of this structure, close to the coast line, the Calatabiano and the Piedimonte faults (PF) can be considered, following Lentini *et al.* (2006), as the neotectonic structures of the basement outcropping in north-eastern Sicily (Fig. 2a).

The western flank of the volcano is affected by a moderate tectonic activity, the Ragalna fault system (RFS) being the main structure (Fig. 2a). This system is formed by three distinct fault segments the Calcerana and the Ragalna faults trending NE-SW and the N–S striking Masseria Cavaliere fault (Azzaro, 1999; Rust and Neri, 1996). This latter structure is a fresh east-facing escarpment up to 20 m high and 5 km long. Less evident compared to the previous one, the NE-SW striking Calcerana fault and the NE-SW trending structure, reported by some authors in the area between Ragalna and Biancavilla, do not show strong field manifestations.

4. Effects connected to the presence of faults

Fault zones are generally characterized by a highly fractured low-velocity belt (damage zone), hundreds of meter wide, bounded by higher-velocity area (host rock) that can broaden for some kilometres (Ben-Zion *et al.* 2003; Ben-Zion and Sammis 2003, 2009 and references therein). Such geometrical setting and impedance contrast is theoretically similar to the well known situations, widely studied in engineering geology and seismology, when soft sediments overly stiff rock. In the presently depicted case, the discontinuity is almost vertically oriented and, as described by Irikura and Kawanaka (1980), it is in principle proficient to produce local amplification of ground motion (Peng and Ben-Zion, 2006; Calderoni *et al*., 2010; Cultrera *et al*., 2003; Seeber *et al*., 2000), as well as to support the development of fault zone trapped waves (e.g. Li *et al*., 1994; Mizuno and Nishigami, 2006).

There is a large number of papers that describe propagation properties of fault-guided waves in terms of ground motion amplification having a propensity to be maximum along the fault-parallel direction. These observations, both in theoretical and experimental approaches deal with almost pure strike slip faults such as the S. Andreas and the Anatolian faults (see Li *et al*., 2000; Ben Zion *et al*., 2003). In the Anatolian fault, Ben Zion *et al*. (2003) observed fault guided waves and an almost constant time delay in the shear waves arrival for different epicentral distances. The authors interpreted such observation as a consequence of a trapping mechanism in the shallower part of the fault between the first 3 and 5 kilometers. Lewis *et al*. (2005) come to a comparable conclusion through the observation of hundreds of seismograms of small magnitude events recorded close to the San Jacinto fault in California. In Italy, Rovelli *et al*. (2002), investigating the Nocera Umbra fault, observed a shallow trapping zone (1-1.5 km) with evidence of measurable amplification effects, as well as pronounced polarization of the ground motion in a direction parallel to the fault strike. On the other hand, Boore *et al*. (2004) in the Calaveras fault, California, noticed that directional effects observed during earthquakes, were occurring parallel to the fault strike and not perpendicularly as it would be expected for a strike-slip mechanism of faulting. Studies about local seismic response nearby fault zones have been performed in Italy and in California by Cultrera *et al*. (2003), Calderoni *et al*. (2010), Pischiutta *et al*. (2012) who observed evidence of ground motion amplification in the fault zone environments and strong directional effects with high angle to the fault strike. Similar studies, performed by Rigano *et al*. (2008) and Di Giulio *et al*. (2009) documented the presence of a systematic polarization of horizontal ground motion, near faults located on the eastern part of the Etnean area, that was never coincident with the strike of the tectonic structures. These directional effects were observed both during local and regional earthquakes, as well as using ambient noise measurements, therefore suggesting the use of microtremors for investigating ground motion polarization properties along and across the main tectonic structures.

In the present study, the results of studies performed in the Etnean area and in South eastern Sicily by Rigano and Lombardo (2005), Lombardo and Rigano (2006), Rigano *et al*. (2008), Di Giulio *et al*. (2009) will be briefly summarized and the outcomes from new investigations carried out in fault areas located both in the Etnean area and in Malta will be shown. Moreover, several measurements were performed in areas significantly distant from the studied tectonic structures (Piano dei Grilli, Etna and the Malta area), in order to observe how directional effects can change at increasing distance from the fault lines.

4.1. Results and discussion

In Figure 3, some examples of polarization plots obtained by Rigano *et al*. (2008), from microtremor measurements performed along and across the Pernicana and Tremestieri faults, are reported. The authors analyzed both earthquake and ambient noise records and found that in all investigated sites the ground motion polarization azimuths were principally NW-SE and NE-SW oriented, for the Pernicana (Fig. 3a) and the Tremestieri (Fig. 3b) faults respectively. It is interesting to observe that such directions were never found coincident with the strike of the investigated faults. Tests were also performed by the authors in order to verify that the observed polarizations were not affected by features of local sources, such as the volcanic tremor, and were stable in time.

The new ambient noise measurements described in the present study, were performed along four short profiles, having recording points spaced about 50m from each other, crossing the Masseria Cavaliere and the Ragalna fault (see respectively Tr#1, Tr#2 and Tr#3, Tr#4 in Fig. 4a). Results of directional effects investigations (Fig. 5) show that at these sampling sites, located in close proximity to the tectonic structures, the H/V spectral ratios have a tendency to increase in amplitude, in the frequency range 1.0-6.0 Hz, at angles of about 80°-90° for Masseria Cavaliere and 60°-70° for Ragalna faults (specify whether angles are from N, or with fault trace). In general, H/V spectral ratios show a broad band frequency effect with multiple adjacent peaks pointing out a preferential direction which is the typical behavior of directional resonances.

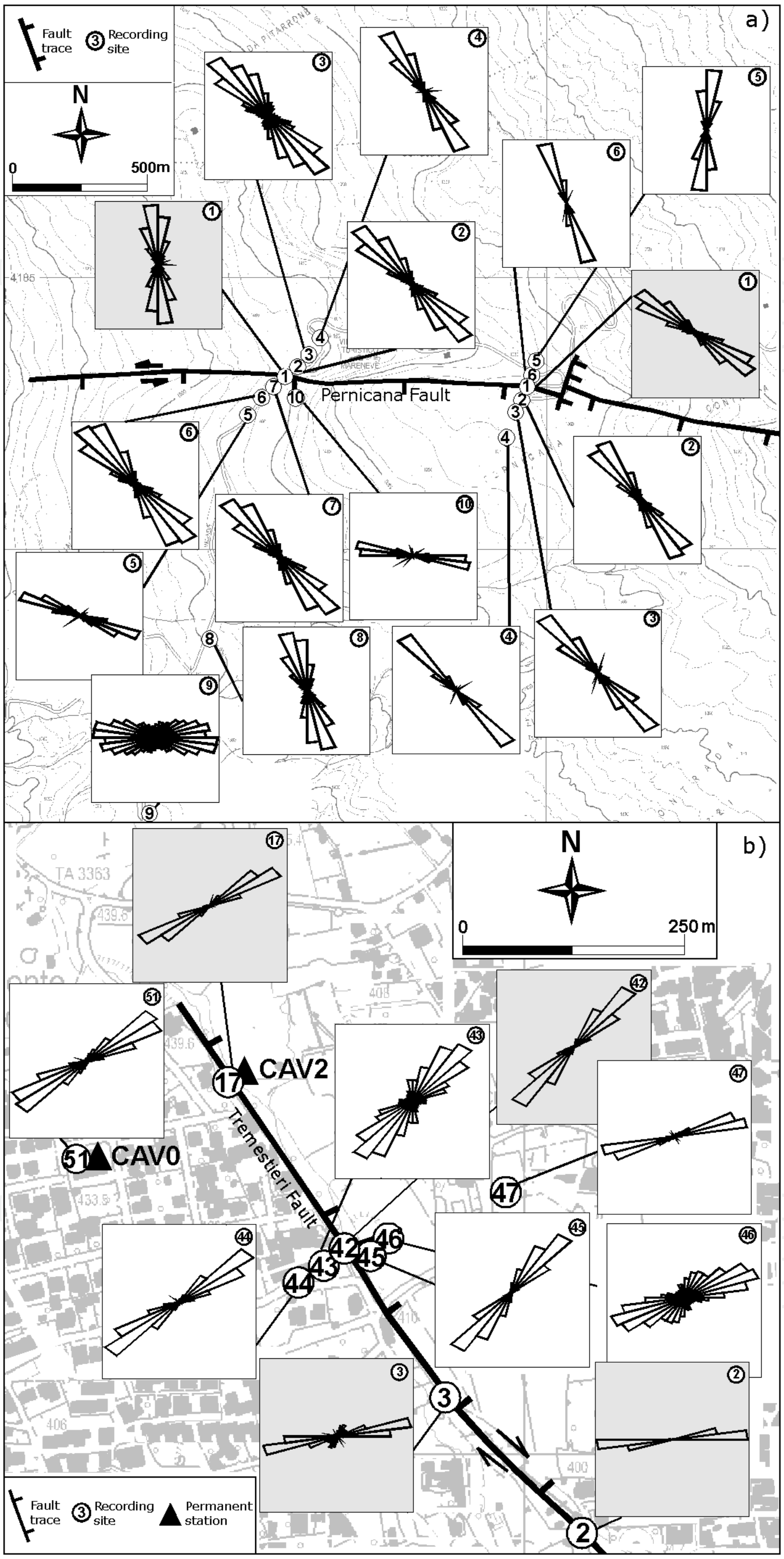

Figure 3. Examples of horizontal polarization angles obtained from ambient noise recorded along and nearby the Pernicana (a) and the Tremestieri (b) faults (modified from Rigano *et al*., 2008).

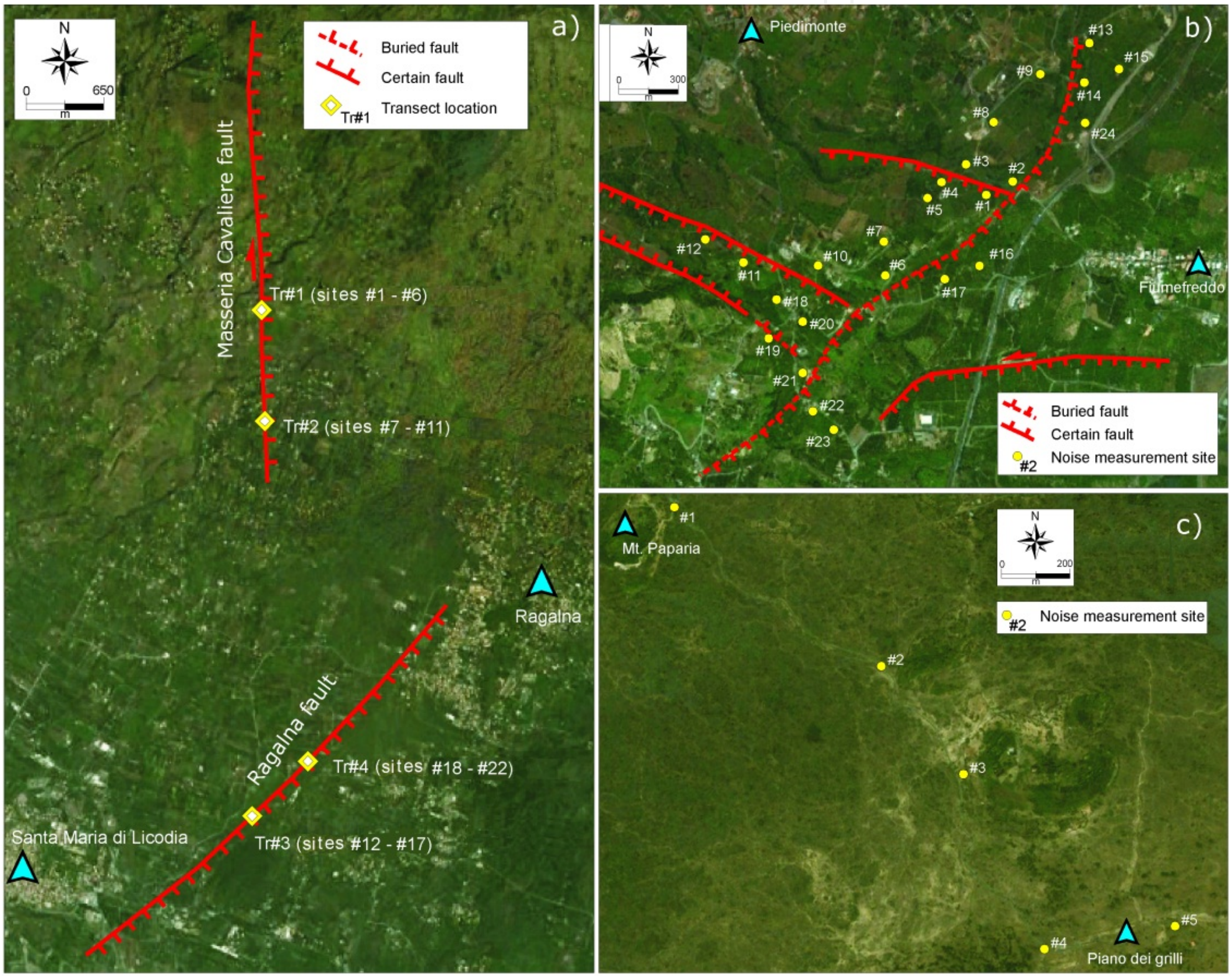

Figure 4. Location of the noise measurement sites. a) transects performed on the Ragalna fault system; b) measurement points on the Piedimonte fault; c) ambient noise recording sites in an area far from the investigated faults.

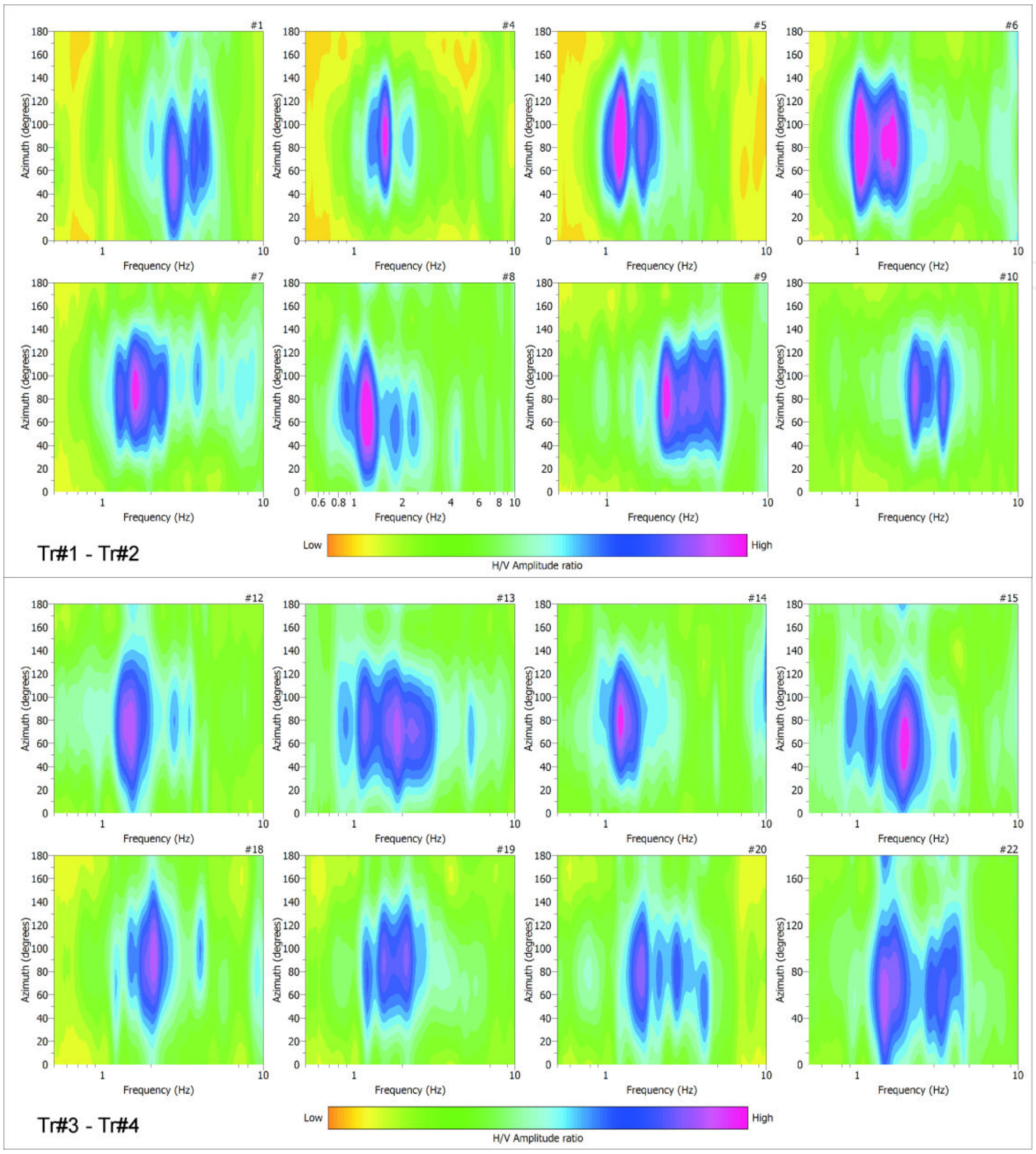

Figure 5. Examples of the contours of the geometric mean of the spectral ratios as a function of frequency (x axis) and direction of motion (y axis) obtained at selected ambient noise recording sites located on the Tr#1, Tr#2, Tr#3 and Tr#4 transects performed on the masseria Cavaliere and the Ragalna fault, respectively.

In order to better quantify the horizontal polarization of the ground motion, the covariance matrix method in the time and in the time-frequency domain were applied (Fig. 6). The results give a clear indication that ambient noise is affected by a significant horizontal polarization at the measurement sites along and across the investigated faults. It is interesting to observe that results obtained through the TF method clearly show that the recorded ambient noise is polarized in a narrow frequency band (1.0-6.0 Hz), following a roughly east-west and north-east-southwest trend, for the Masseria Cavaliere and the Ragalna faults respectively. The TD results confirm the same polarization trend although in some cases the rose diagrams show polarizations that are not sharply oriented (see e.g. #1, #2, #16 and #17, in Fig. 6). It is in our opinion clear that possible contributions of high-frequency noise (6.0-10.0 Hz), related to transients or to small scale geologic heterogeneities of a site, may imply incorrect results as shown for instance in Figure 7 where the TD rose diagrams dramatically change their polarization directions whereas the TF polar diagrams indicate that changes occur at higher frequencies only.

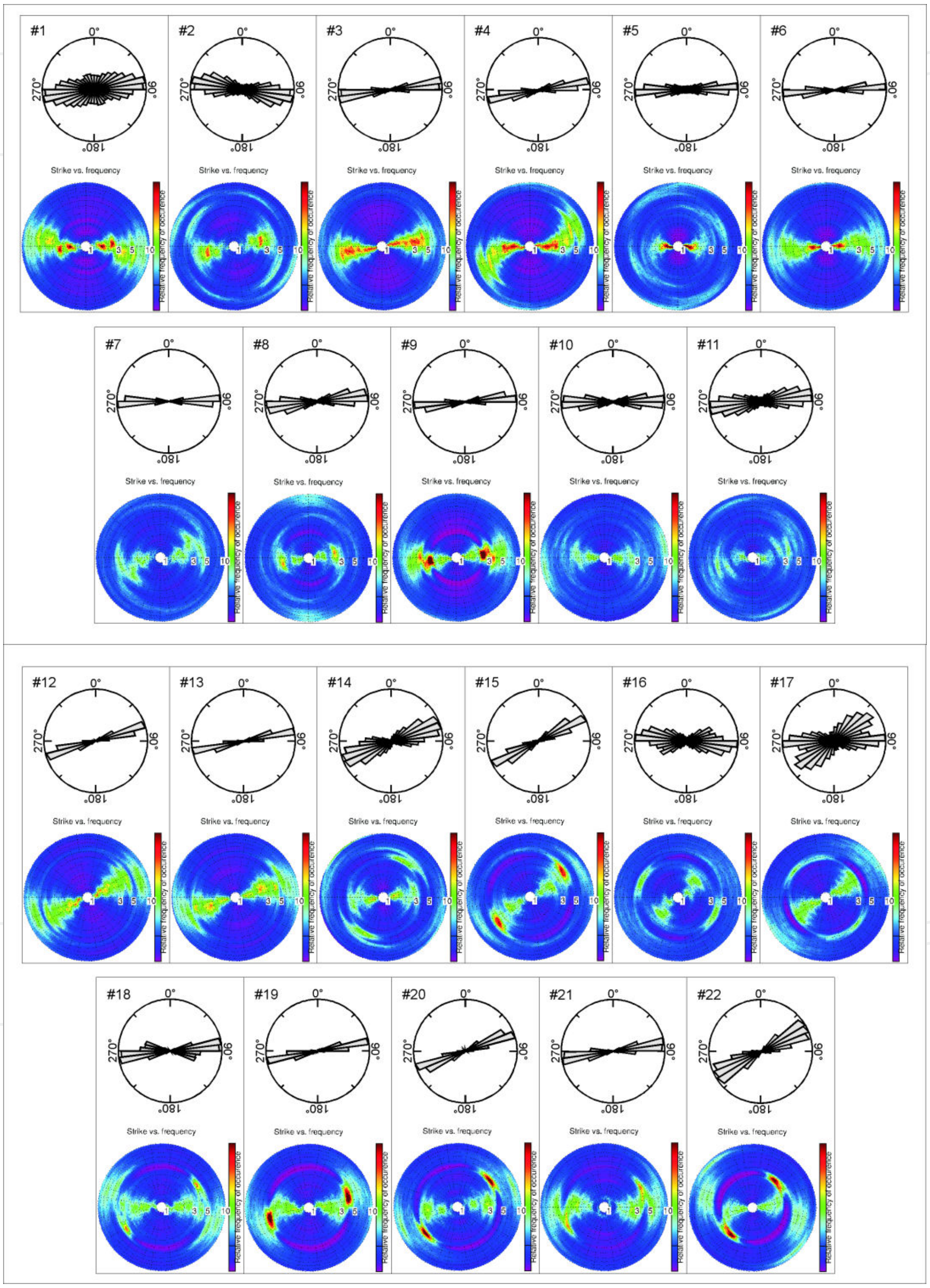

Figure 6. Results of horizontal polarization angles computed through the TD (rose diagrams) and TF analysis considering the frequency range of 1.0-10.0 Hz (polar plots), for Ragalna fault system.

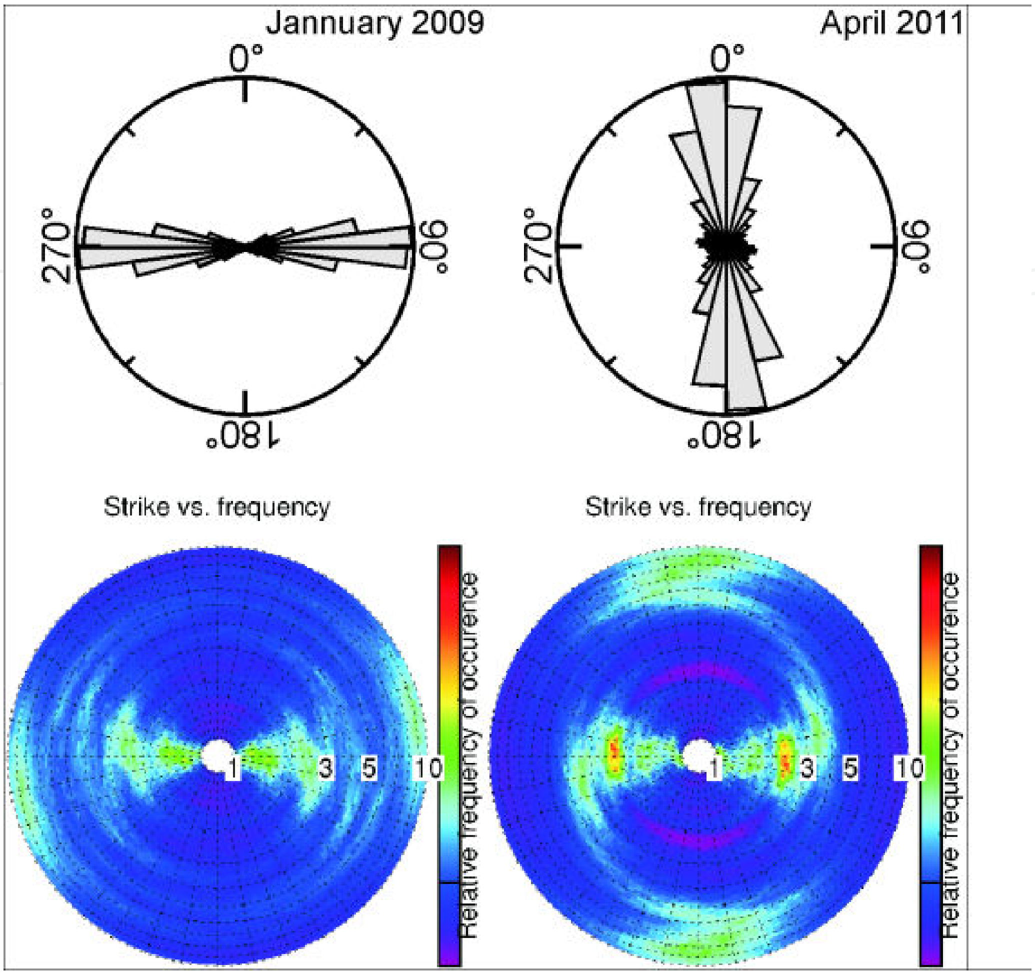

Figure 7. Polarization test on the measurements performed in two different periods (January 2009 and April 2011) in the site #10 of the transect Tr#2 of the Masseria Cavaliere fault.

The other important structure that we investigated is the Piedimonte fault system (PF). The major fault, striking ENE-WSW, is located at the end of the Pernicana fault. It seems to represent an old structural element with a marked morphologic scarp, but no evidence of activity in historical times (Azzaro *et al.*, 2012). The minor faults which spread out from the main structure, striking mostly WNW-ESE, are related with the movement affecting the Pernicana fault. The directional resonance plots (Fig. 8), obtained by rotating the NS and EW components of motion seems to highlight the presence of two different structural behaviors. The results of measurements performed on the footwall of the fault (Fig. 8a) highlight strong directional effects in the frequency range 1.0-6.0 Hz with a NE- SW strike. In the hanging wall (Fig. 8b) the azimuths, the frequency bands and the amplitudes of the HVNRs vary at each measurement point in relation with the small scale geologic framework of each site. Polarization results (Fig. 9) confirm the frequency range and azimuths observed through the rotated spectral ratios. Indeed, on the footwall of the major Piedimonte fault the recorded ambient noise is polarized in a narrow frequency band (1.0-6.0 Hz), similarly to the faults in the western area of the volcano, but with an angle of about 45°. In the hanging wall a rather scattered distribution of polarizations is observed (e.g. #13, #15, #16, #23).

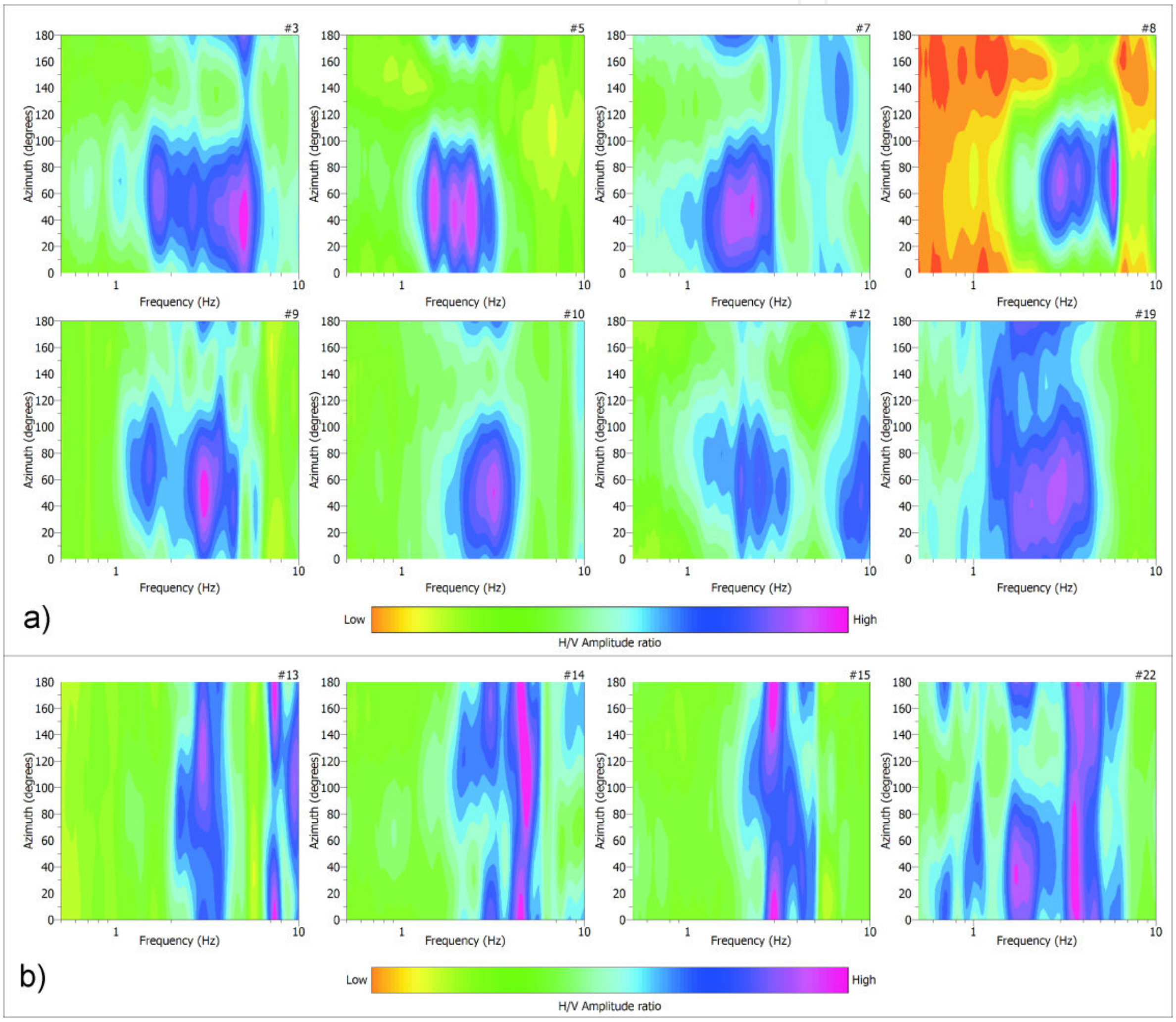

Figure 8. Examples of the contours of the geometric mean of the spectral ratios as a function of frequency (x axis) and direction of motion (y axis) obtained at selected ambient noise recording sites located on the footwall a) and hanging wall b) of the Piedimonte fault.

http://dx.doi.org/10.5772/55439

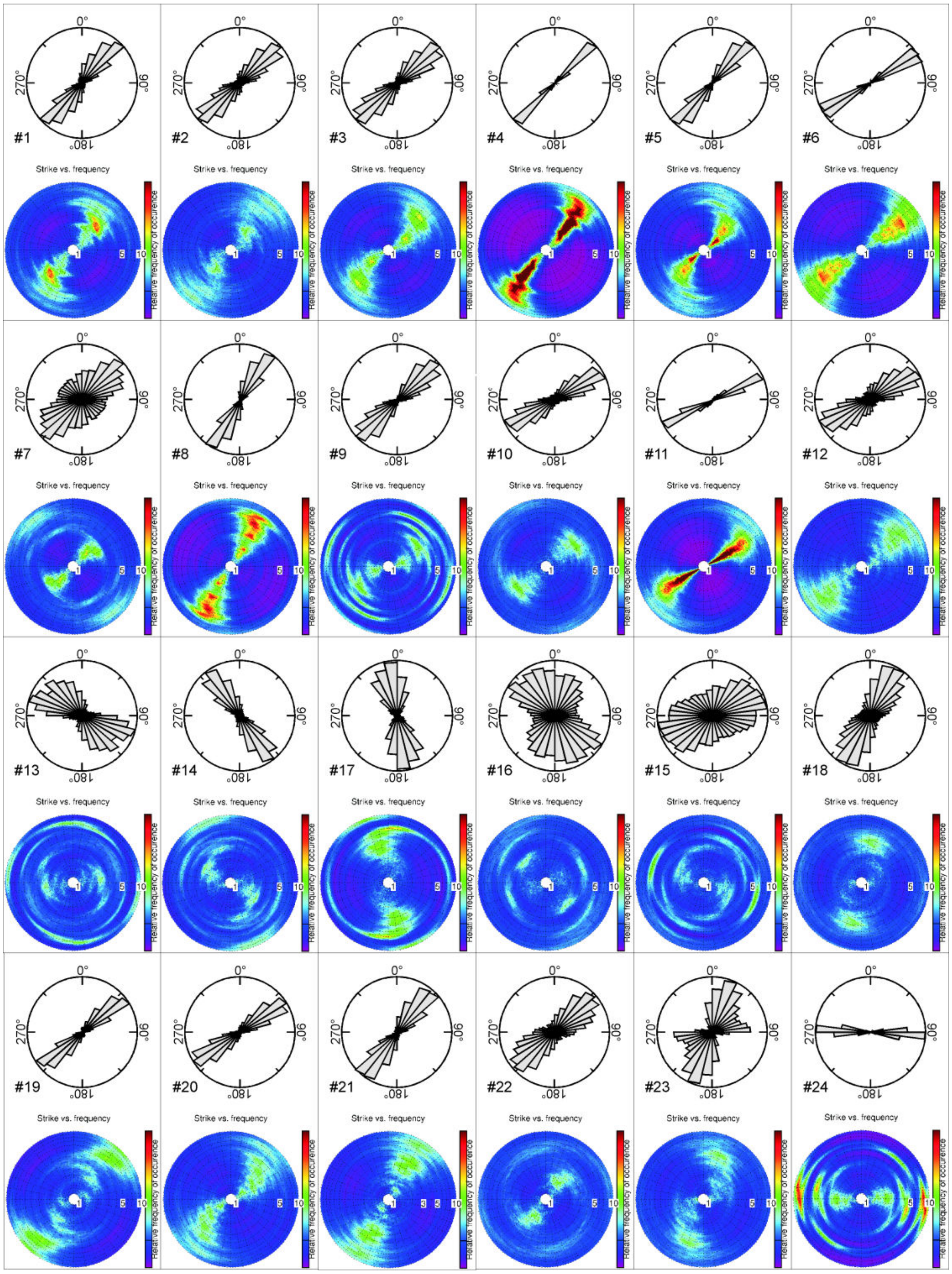

Figure 9. Horizontal polarization angles computed through the TD (rose diagrams) and TF analysis considering the frequency range of 1.0-10.0 Hz (polar plots), for the Piedimonte fault.

Ambient noise recordings were also performed in some fault segments belonging to the Great Fault system of the Malta area, in order to investigate site effect features of tectonic structures located in a non volcanic area. Results obtained (Fig. 10) indicate the existence of directional effects similar to those found in the investigated Etnean structures, although a slightly more complicated pattern, probably linked to the influence of the complex lithology existing at both sides of the fault, is observed. However, the polarization plots obtained from records near the fault show a prevailing direction that is not parallel to the structure strike.

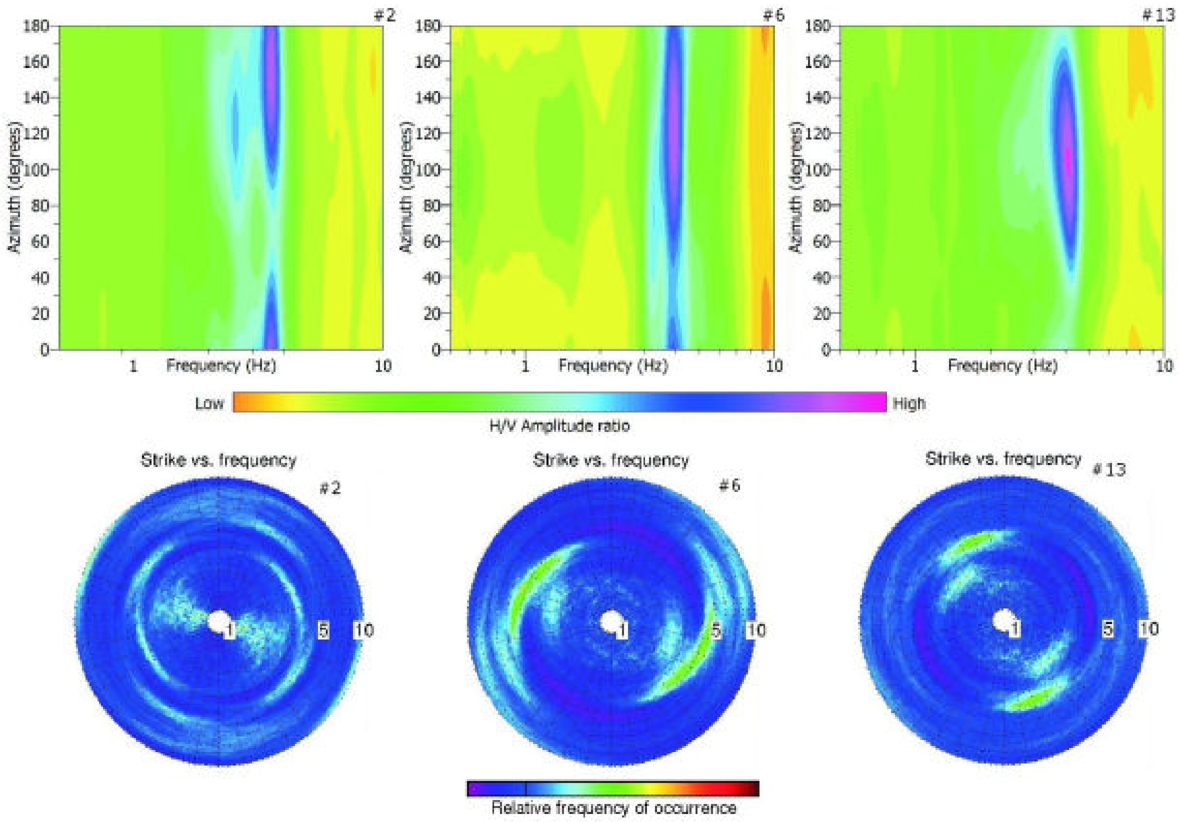

Figure 10. Examples of directional resonances and horizontal polarization azimuths obtained at selected ambient noise recording sites located on the Malta Great Fault system.

It is not an easy task to interpret all experimental observations when these exhibit prevailing polarization directions that are sharply changing and are always non-coincident with the fault strike. In a recent paper, Pischiutta *et al*. (2012), find that the mean polarization azimuth turns out to be perpendicular to the expected synthetic cleavages. We have to remember that four types of fractures can develop in fault zone (Riedel, 1929; Tchalenko, 1968): a) extensional fracture (T); b) synthetic cleavage (R); c) antithetic cleavage (R'); d) pressure solution surfaces (P). The orientation of these fractures depends on the direction of the resulting stress localized around the fault. Therefore, an interpretation of the present results could, in our opinion, be proposed by focusing our findings in the frame of the brittle rheology of the hosting rock (Pischiutta *et al*., 2012).

http://dx.doi.org/10.5772/55439

Finally, tests were performed to check if the observed directional effects keep the same orientation in areas significantly distant from fault lines. For this reason, ambient noise was recorded in the PG (Piano dei Grill) area, located in the western flank of Mt. Etna, as well as in an area in the northern Malta island. The results (Fig. 11) show that ground motion directions coming from both rotated spectral ratios and polarization diagrams tend to become randomly distributed and/or uniformly scattered. Such findings further support the observations of Rigano and Lombardo (2005) that performed ambient noise measurements in proximity and at few kilometers distance from the Mt. Tauro fault, located in south-eastern Sicily (Fig. 12).

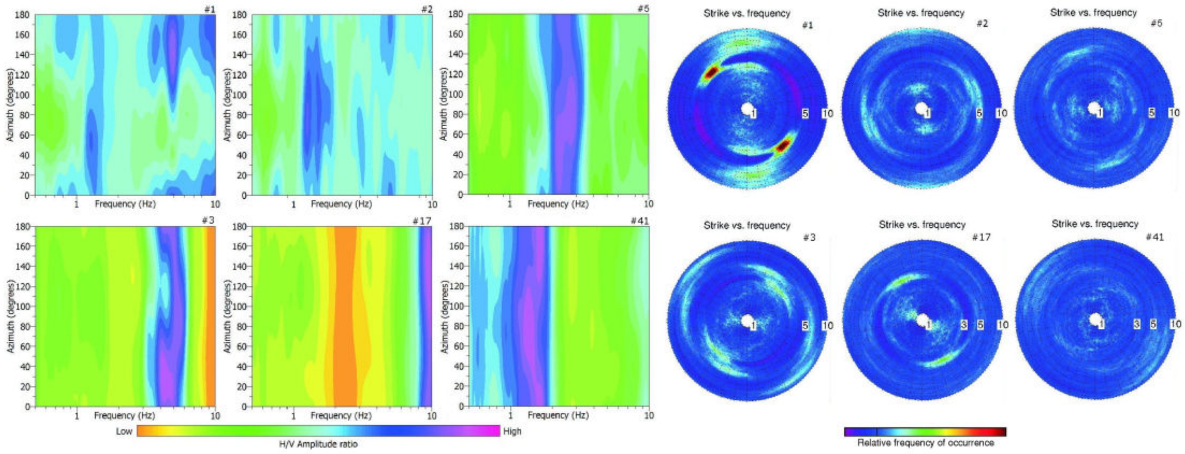

Figure 11. Examples of directional resonances and horizontal polarization azimuths obtained at selected ambient noise recording sites located on the PG area (#1, #2, #5) and in the northern Malta area (#3, #17, #41).

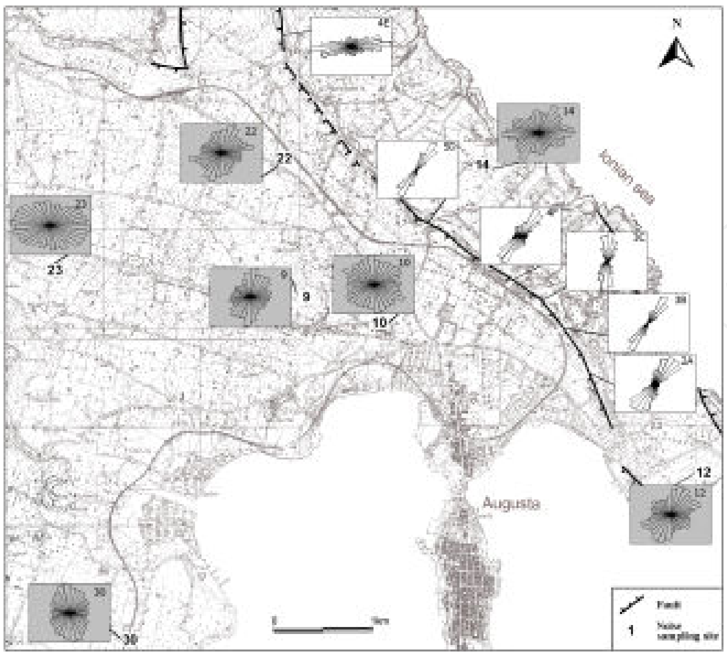

Figure 12. Ambient noise polarization plots in the Augusta area (modified from Rigano and Lombardo, 2005).

The outcomes of the present research allowed us to draw the following considerations:

- In the neighborhood of fault areas, the presence of a damage zone implies the existence of ground motion amplifications and persistent directional effects of the horizontal component of motion, set into evidence by both earthquake and ambient noise records, that are observed till several hundred meters distance from the fault line;
- The directional site effects and the polarization angles observed for all the investigated structures are always non-parallel to the fault strike making a simple explanation in terms of fault-trapped waves not convincing. To attempt a possible explanation for this recurrent ground motion property we postulate the existence of a tight relationship with the expected synthetic cleavages.
- The directional resonance and the TF polarization analysis set into evidence that fault effects appear concentrated in the frequency range 1.0-6.0 Hz. The stability of this frequency interval, observed both in the western and in the eastern flanks of the volcano, encourage us to affirm that it is a possible marker for observing site effects in fault zones, at least in the Etnean area.
- Polarization directions coming from both rotated spectral ratios and polarization diagrams tend to become randomly distributed and/or uniformly scattered when noise measurements are performed in areas where no fault s are evident.

Finally, it seems important to point out that present results give further support to findings from previous studies (e.g. Rigano *et al*., 2008; Di Giulio *et al*., 2009; Pischiutta *et al*., 2012) concerning site effects in fault zones and promote the use of ambient noise recordings as a fast technique for preliminary investigations about angular relations between fractures field and directions of amplified ground motion and for preliminary quick surveys in area where the urbanization or the presence of shallow sedimentary deposits hide the evidence of tectonic structures.

5. Site effects linked to the presence of cavities

The presence of either natural or artificial cavities in the shallower part of various lithotypes is an important aspect whose effects, in terms of the local seismic response evaluation, are still not fully investigated. Grottos can originate from different processes and affect rocky lithotypes that at the surface appear very stiff and characterized by good elastic properties. It is for instance possible to observe the development of cavities, several meters wide and hundreds of meters long, inside basaltic lava flows, that are related to the cooling of the shallower part of lavas while the still fluid portion flows underneath. Also typical is the presence of extensive cavities in calcareous formations, due to the development of karstic phenomena. Local seismic effects related to such conditions therefore need to be investigatedsince, although the lithology often belongs to the bedrock type, they cannot be considered free from significant modifications of both amplitude and frequency content of the seismic input.

The scientific literature concerning these phenomena is rather poor. Studies were performed by Nunziata *et al*. (1999) in some cavities existing inside the pyroclastic terrains of the Napoli downtown area where the authors observed, through numerical modeling, an amplitude decrease of the ground motion at the top of the investigated cavities. Experimental studies, using both earthquake and ambient noise records were recently performed in south-eastern Sicily by Lombardo and Rigano (2010) and Sgarlato *et al*. (2011) and their results will now be briefly summarized.

The influence of cavities in the evaluation of the local seismic response was studied in some selected sites located in the Hyblean region (in the cities of Lentini, Melilli, Siracusa and Modica) and the urban area of Catania, taking into account both natural and artificial cavities such as railway tunnels. In total, the measurements were carried out in about fifteen cavities. They were selected according to criteria of relatively easy access, different geometric features and possibility of having detailed underground surveys. The majority of the investigated grottoes develops in heavily urbanised areas and in some cases, houses and small edifices are built over, or neighbouring them. About 400 time histories of microtremors were recorded in 90 measurements sites that were located inside and over the vault of each grotto, as well as in its neighbourhood, along short profiles having a few tens of meters length, evaluating the horizontal-to-vertical noise spectral ratio as well as the polarization angle of the horizontal component of motion. Besides, in the Catania area, a cavity (Petralia grotto) was selected to install four seismic stations for recording earthquakes. The grotto is located in the northern part of Catania and roughly trends in E–W direction. It develops at a depth of about 3 m from the topographic surface where its easternmost part is open (Fig. 13). Its cross section has a variable size ranging between 10 and 15 m in width and is about 2.5 m high on average. This cavity is formed by several chambers connected by tight passages and it shows evidence of several collapses, the first of which took place at a few tens of meters from the opening of the cavity. Its origin is connected to the flow, cooling and drainage of a pre-historical Etnean lava that, similarly to other lava flows have covered, till historical times, the Catania urban area terrains. The stations were deployed inside, over the vault, in the vicinity of the grotto (named *incave*, *upcave* e *outcave*, respectively) and in a reference site (*uni*), about 500 m away, located on the bedrock. Data were processed using the earthquake's horizontal to vertical spectral ratio (HVSR) or receiver function technique, and the standard spectral ratio (SSR) to a reference site. A set of 34 seismic events, showing a good signal-to-noise ratio were recorded for five months.

5.1. Results and discussion

Examples of the HVNR results obtained in the various investigated cavities are reported in Fig. 14a. As the plots summarize, it is not possible to observe a unique behavior. The results show the lack of H/V spectral ratio peaks inside some cavities, as shown in the examples #6, and #1* where spectral ratio peaks do not reach the amplitude of three units. On the other hand, H/V obtained from measurements performed in some other cavities (#1, #3, #2* and #3*) tend to reach a significant amplitude (>2 units) in some frequency bands. Such behavior appears related to the size of each cavity. It is in fact observed that a tendency towards H/V significant peaks is evident in cavities whose height is not less than 3-4 metres. It is also

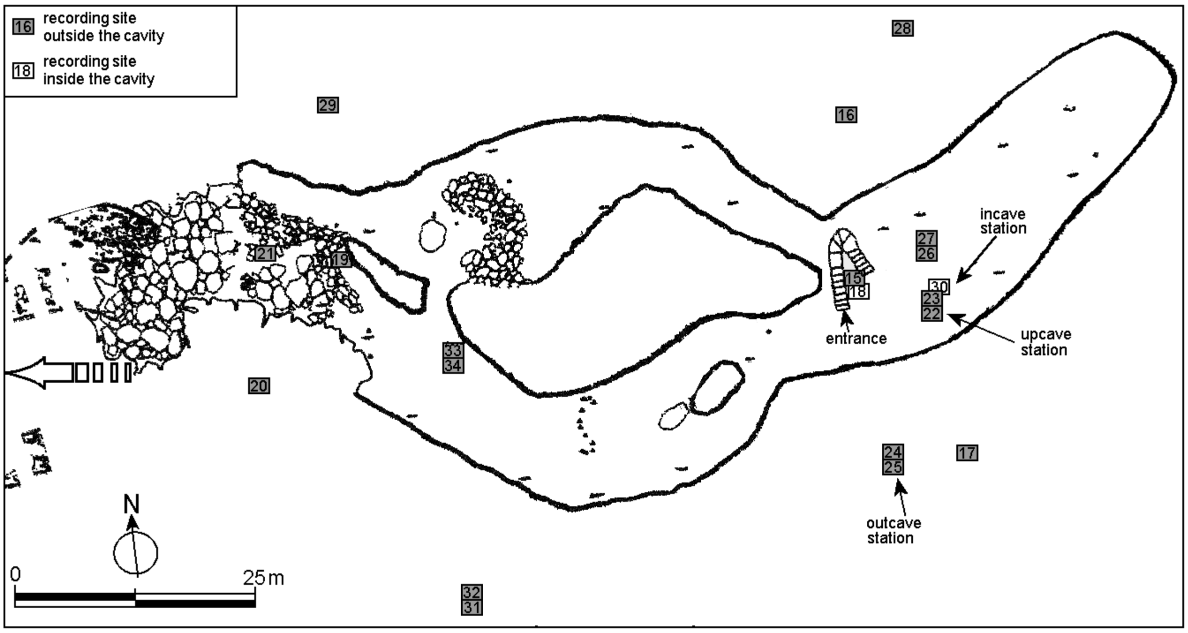

Figure 13. Sketch map of the eastern end of the Petralia grotto and location of permanent and mobile stations; white and grey squares refer to ambient noise recording sites located respectively inside or over and outside the grotto.

interesting to note that in some cases considerable effects are observed in H/V spectral ratios from measurements performed over the vault of the cavity (i.e. #3, #3*), while in other cases (#1 and #2*) pronounced peaks are observed in measurements performed both inside and over the grotto.

Some interesting considerations can be inferred from investigating possible directional effects. The plots in Fig. 14b show that the peaks centered at 2.5 Hz and 1.5 Hz, for cavities #1 and #2* respectively, as well as the peak in the range 4.0 – 6.0 Hz, observed for the cavities #6 and #3*, are markedly directional. The peak values increase up to 3 - 4 units, at directions of 90° and 180° that are nearly coincident with the strikes of the investigated cavities (see the strikes reported in the panels of Fig. 14a).

No.	Name	Locality	H (m)	No.	Name	Locality	H (m)
1	Della Chiesa	Catania	5	1*	De Cristoforis	Lentini	2
2	Micio Conti	Catania	3	2*	C.le Palma	Lentini	5
3	Di Bella	Catania	8	3*	Speri	Lentini	6
4	Caflish	Catania	2	1	Ipogeo	Siracusa	8
5	Ciancio	Catania	4	1	Mastro Pietro	Melilli	8
6	Petralia	Catania	2	1	Barriera	Melilli	10
7	Novalucello	Catania	1	1	Cava	Modica	6
8	Magna	Catania	2.5				

Table 1. List of investigated cavities.

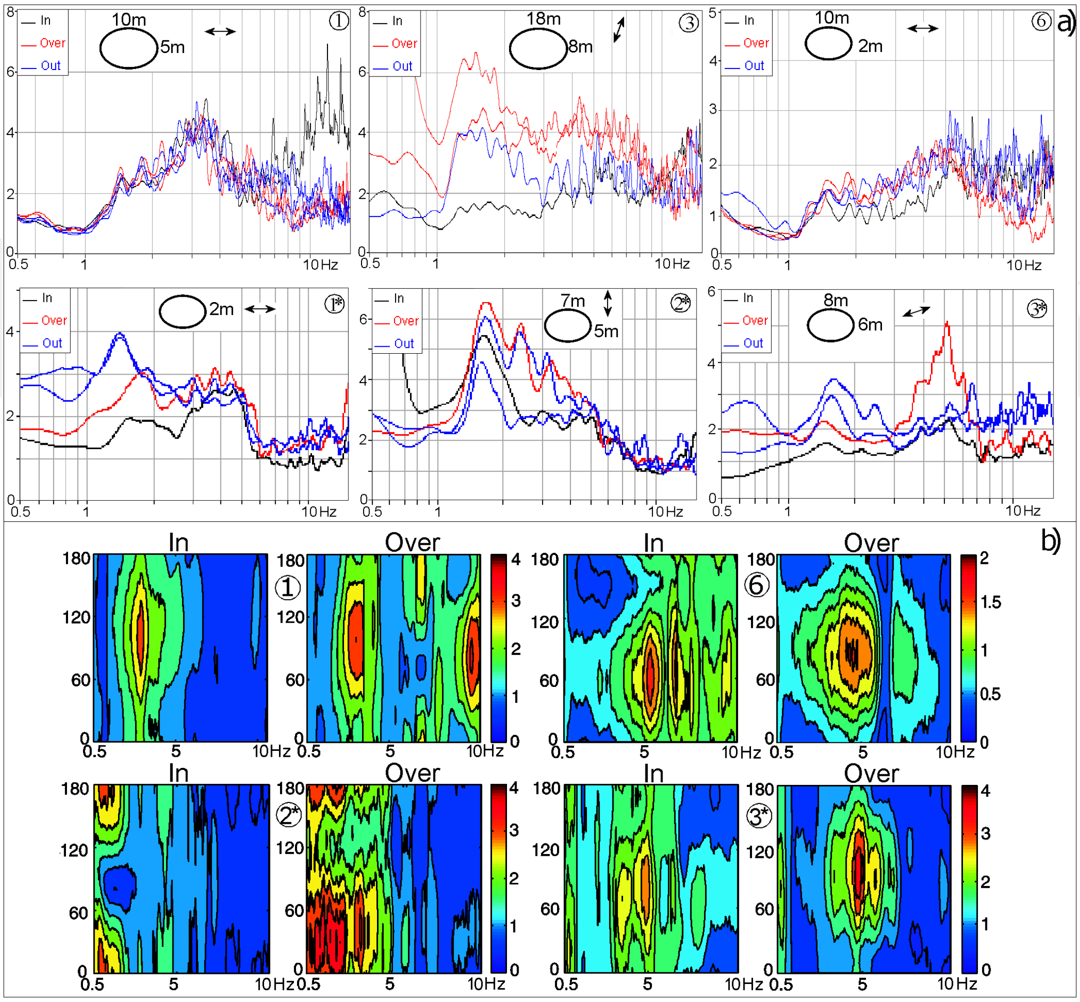

Figure 14. a) H/V spectral ratios obtained from ambient noise measurements performed in different grottoes (numbers refer to the grottoes listed in Tab. 1); the ellipse represents the dimensions of the vertical section of each cavity while the arrows indicate in which direction the grotto develops underground. (b) Contours of the geometric mean of ambient noise spectral ratios as a function of frequency (x-axis) and direction of motion (y-axis) for recordings performed at *Della Chiesa* (# 1), *Petralia* (# 6), *C.le Palma* (# 2*) and *Speri* (# 3*) grottoes.

To validate the reliability of these ambient noise measurements, a comparison was made with findings from the HVSR and SSR of earthquake data recorded in a test site (Petralia grotto). All spectral ratios (Fig. 15a, b) obtained from records at incave, upcave and outcave stations, show moderate peaks that reach at most a value of 3 units. The HVSR show peaks in two frequency ranges, namely 1.2–1.8 Hz and 3.0–7.0 Hz. It has to be noted that in complex situations the identification of main resonance frequencies through HVSR analysis can be biased by the presence of deamplification phenomena in the vertical component of the ground motion. For this reason the ratios between the vertical component spectra of records at the local permanent stations and at the reference one were calculated (Fig. 15c) in order to highlight the frequency band at which the results can be considered reliable. In Fig. 15c no evident deamplification phenomena are observed, but the vertical component at outcave station, especially in the frequency range 3.0 – 7.0 Hz, shows a slight tendency to deamplification which could explain the spectral peaks observed, in the same frequency range, in the HVSR. The comparison of HVSR obtained at the three sites shows a tendency toward slightly more pronounced peaks at outcave station with respect to stations located both over and inside the cavity, the last one, in particular, showing always smaller spectral peaks for the EW component in the frequency band 3.0–7.0 Hz (Fig. 15a). A similar behavior is also observed in the SSR (Fig. 15b) where the spectral ratios obtained for the incave station show, especially in the same frequency range, smaller amplifications in both EW and NS components. Such a tendency is also shown in the results of ambient noise measurements (Fig. 15d and e). Moreover, it is interesting to point out that both HVSR and HVNR show, at upcave station, a striking amplitude decrease, in the frequency band 7.0–10.0 Hz, of EW component of motion (see Fig. 15a, d, e). Such behavior appears related to the amplitude increase of the vertical component of motion at the upcave station, as confirmed by the V/Vref shown in Fig. 15c. This implies that, at highest frequencies, both the HVSR and the HVNR show higher values at incave station rather than at upcave station. On the other hand, being evident that in the above mentioned frequency band, at upcave station the EW component of motion has a low amplitude, the SSR shows also a striking decrement (Fig. 15b) and the spectral ratios at incave are lower than the same spectral ratios obtained at upcave. This last observation is a consequence of the low amplitude values at the denominator of the SSR, with respect to that of HVSR, as expected for the horizontal component of motion at the reference site. The SSR however shows amplification mostly in the range 3.0–7.0 Hz (Fig. 15b).

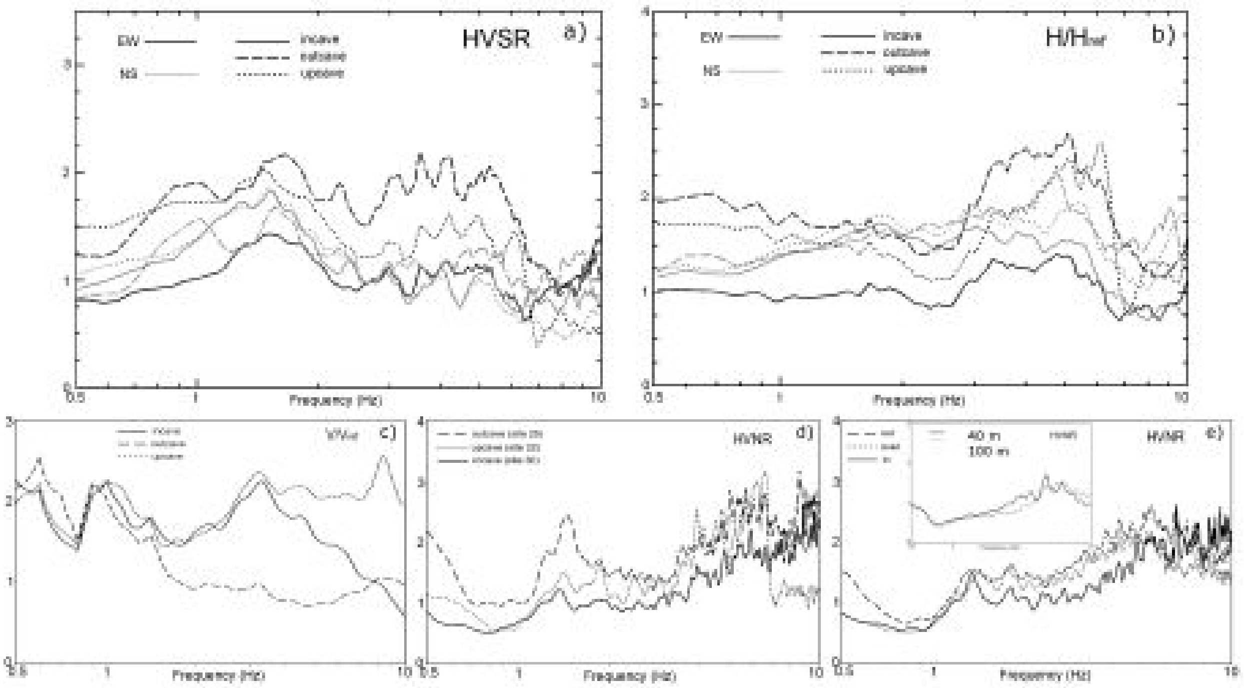

Figure 15. Spectral ratios HVSR (a) and standard spectral ratios SSR (b) of all events recorded at Petralia grotto; V/Vref) of the vertical component of seismic events recorded at the local permanent stations and at the reference one (c); HVNR recorded at the sites of permanent stations (d) and average of all measurements performed in different sites located inside, over and outside the investigated grotto (e), the location of all recording sites is shown in Fig. 14. The inset shows the HVNR from ambient noise recorded in two sites located at distance of about 40m (grey curve) and 100 m (black curve) from the grotto.

Other noise measurements were performed to the south of the cavity at distances of about 40 m and 100 m from the cavity entrance in order to test how the spectral features previously described appear at increasing distance from the grotto. The obtained HVNR (see inset in Fig. 15e) shows that the 1.2-1.6 Hz spectral ratio peaks disappear already at a distance of about 40 m from the cavity, therefore indicating that they seem to belong mostly to specific features of the grotto area. On the other hand, the peaks at 3.0 – 7.0 Hz, although less pronounced, are still observed, implying that they are linked, at least in part, also to structures extending in a wider area around the grotto.

A polarization analysis was performed to investigate directivity effects related to the cavity. The azimuthal directions of the horizontal component of motion were obtained after filtering the signal in three frequency bands (1.0 – 3.0, 3.0 – 7.0 and 7.0 – 10.0 Hz) aiming to investigate the frequency ranges observed in the H/V spectral ratios. It can be clearly observed (Fig. 16) that almost all rose diagrams show a sharp polarization in the EW direction. Only polarizations obtained at the incave station by filtering the signal in the range 1–3 Hz appear highly scattered. Polarization effects were also investigated, using ambient noise records, in the sites located at 40 and 100 m away from Petralia grotto (see bottom panels in Fig. 16). The results obtained show that such polarization effects become less evident as the distance from the cavity increases.

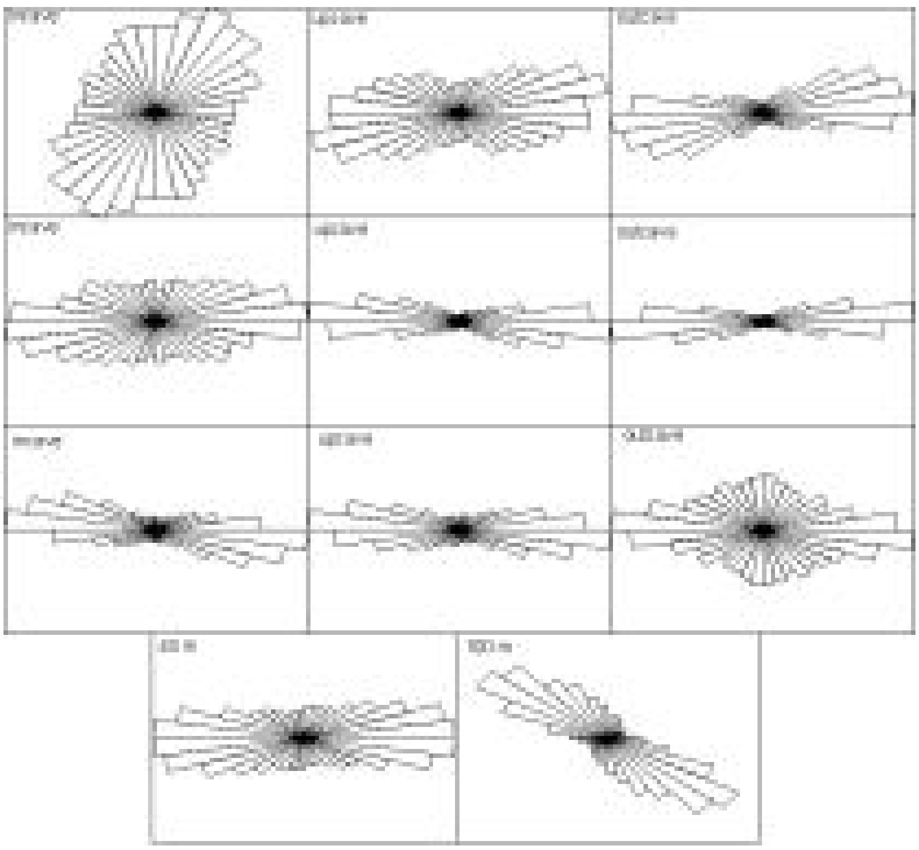

Figure 16. Polarization of the horizontal component of motion obtained by filtering the recorded seismic events at 1.0–3.0 Hz (upper panels), at 3.0–7.0 Hz (middle panels) and 7.0–10.0 Hz (lower panels); the bottom panels refer to polarization from ambient noise measurements performed at sites located 40 and 100 m away from the grotto.

In order to compare the results from recordings in a natural cavity with those from records performed in a cavity having a simpler geometry, ambient noise was also recorded inside, over, and in the neighborhood (≈30 m) of two artificial tunnels. Both tunnels are located close to the Catania urban area, dug at about 4 m from the topographic surface and having a length of about 100 m, but different height. One of them (height of about 4 m) is dug in massive lavas and the other (height of about 7 m) is excavated in altered lavas. HVNRs show that in the smaller tunnel (Fig. 17a), dug in massive lavas, spectral peaks are significantly less pronounced than those observed in the tunnel, dug in altered lavas, having a greater height (Fig. 17b). In this tunnel, H/V spectral peaks, in the frequency range 4.0–7.0 Hz, obtained from measurements performed over and inside, attain values of about 8 and 4 units, respectively, therefore confirming the observation, aforementioned for the Petralia grotto, that inside the cavity spectral peaks are less pronounced than those observed when measurement is performed over the cavity. It is noteworthy that the spectral ratios from measurements in both tunnels show peaks that however are more pronounced than those observed from H/V performed in and over the study grotto. This is possibly related to the height that in both tunnels is significantly greater than in the studied cavity, considering also that the lava characteristics (altered lavas) of the Petralia grotto area are comparable to those of the lava where the greater artificial tunnel is dug.

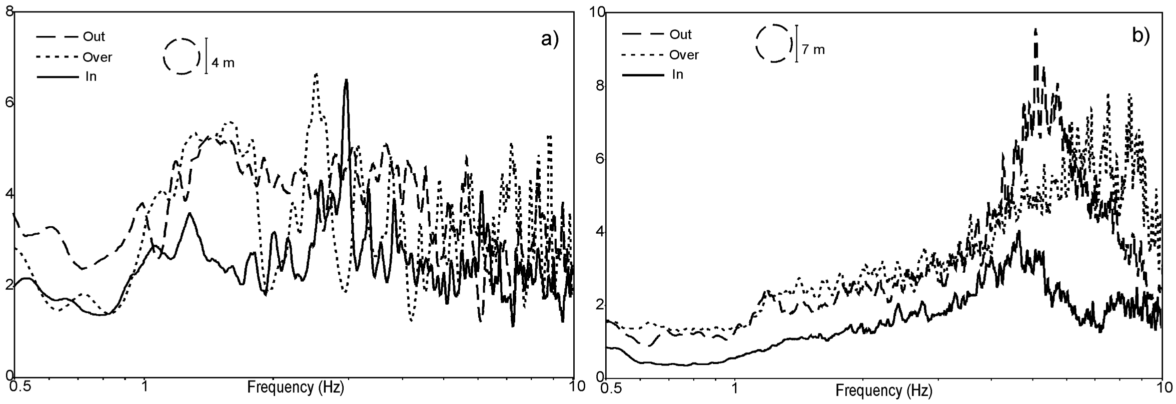

Figure 17. Spectral ratios HVNR from measurements performed in two underground tunnels having different height.

The results so far described are quite complex but nevertheless some interesting considerations can be inferred:

- The size of the vertical section and geometry of the cavities seem to play an important role. According to experimental data, it appears evident that only cavities having height greater than about 4 meters show significant H/V spectral peaks.
- Results of spectral ratios at Petralia grotto (having height of about 2.5 m) show spectral ratio peaks less pronounced than those observed in grottoes and tunnels having height of about 4 and 7 m. Such behavior, in our opinion, need to be tested and interpreted with the support of numerical modeling, to investigate also about possible amplifications/deamplification of the vertical component of motion as highlighted by processing earthquake data.

- Findings from HVSR and SSR at the test site #6 point out the lack, or the modest presence, of amplification effects at the recording site located inside the cavity with respect to stations placed over and outside the grotto. This effect could be explained in the frame of the constructive interferences between direct and reflected waves that can take place at the free surface, so that, as it would be generally expected, a decrement of amplitude oscillations can be observed at depth.

- In all investigated cavities, significant directivity effects were observed, pointing to the existence of a marked polarization of the horizontal component of the ground motion in a direction parallel to the main axis of the grotto. Such evidence is not negligible in the planning of buildings to be erected in the neighboring areas. It is however remarkable that experimental data show that at distances greater than about 100 m from the cavity, the polarization analysis shows azimuths no more coincident with the strike of the grotto.

It is however important to denote that further investigations need to be performed in other cavities having various height, performing also 2D/3D modeling in order to simulate the variations that a wavefront undergoes when propagating through a terrain having a strong impedance contrast due to the existence of a hollow space.

6. Site effects in landslide zones

Landslide phenomena, besides exposing the affected areas to a considerable natural risk, imply the occurrence of significant variations in the local seismic response. To investigate such features, Fekruna Bay, in the area of Xemxija (Fig. 18), was selected. Xemxija is a seaside village and marina on the northeastern part of Malta and it is a very important site for touristic attractions, as well as cultural and historical heritage. The study area spans a couple of square kilometres. More than half of it is intensely built, while the remaining area consists of meadows and agricultural land. The area is characterized by a geology and topography that varies over small spatial scales. Its geomorphologic features are the result of the combined effect of the lithology, tectonics and coastal nature that shaped the region, and such features contribute towards the degree of geological instability of the whole area and particularly to the cliff sections.

The outcropping local geology in the Fekruna bay (Pedley *et al*., 2002) is characterised by the Upper Coralline Limestone (UCL) and the Blue Clay (BC) formations. Underneath the BC, a carbonatic formation, the Globigerina Limestone formation (GL) consisting mainly of loosely aggregated planktonic foraminifers, and a Lower Coralline Limestone formation (LCL), which consists of massive biogenic limestone beds, are present. This geolithologic sequence gives rise, in the north coast of Malta, to lateral spreading phenomena which take place within the brittle and heavily jointed and faulted UCL formation overlying the BC which consists of softer and unconsolidated material (Mantovani *et al.*, 2012). The UCL formation is characterized by a prominent plateau scarp face, whereas BC produces slopes extending from the base of the UCL scarp face to sea level. It is well known that lateral spreading usually takes place in the

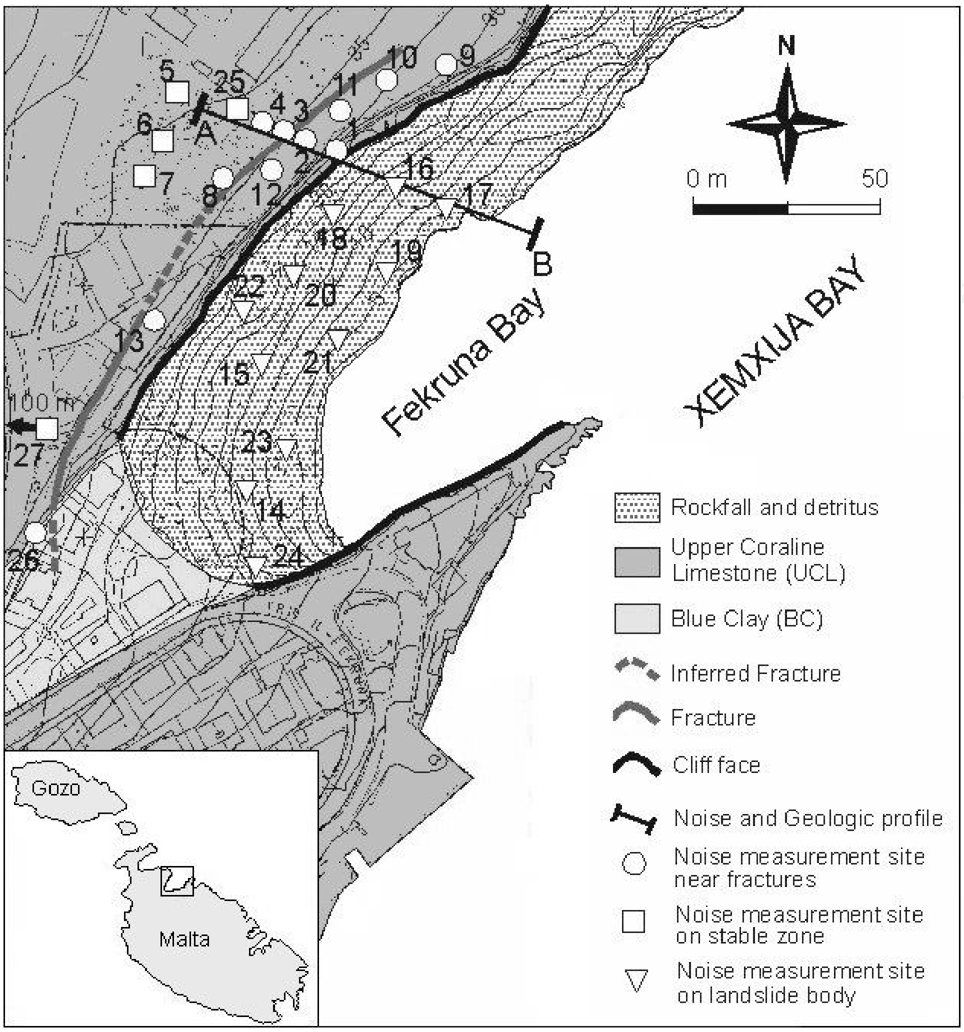

Figure 18. Geo-lithologic map of the north-eastern part of the Xemxija bay (modified from MEPA Various Authors, 2004). The insets show the location of the study area and a sketch of lateral spreading effects along the Xemxija coast.

lateral extension of cohesive rock masses lying over a deforming mass of softer material where the controlling basal shear surface is often not well defined.

A preliminary study of the area, focusing our attention on the risk of landsliding and rockfalls, was carried out using the ambient noise HVNR technique in order to characterize the rock masses behavior in the presence of fractures linked to the landslide body. This type of measurements can be done quickly and with a high spatial density, providing a fast tool for setting the dynamic behavior of the rock outcropping. Generally, this spectral ratio exhibits a peak, corresponding to the fundamental frequency of the site whereas, it is less reliable as regards its amplitude. Nevertheless, the HVNR curve contains valuable information about the underlying structure, especially as concerns the relationship between V_S of the sediments and their thickness (Ibs-Vonseth and Wholenberg 1999; Scherbaum *et al*. 2003). Recordings of ambient noise and the use of the HVNR technique has recently had widespread use in studying landslides (*e.g.* Del Gaudio *et al*., 2008; Burjánek *et al*., 2010; Del Gaudio and Wasowski, 2011; Burjánek *et al*., 2012).

We recorded ambient noise at 27 sites using a 3-component seismometer (Tromino, www.tromino.eu) and directional effects were investigated by rotating the NS and EW components of motion by steps of 10 degrees starting from 0° (north) to 180° (south). Moreover, a direct estimate of the polarization angle by using the covariance matrix method (Jurkevics, 1988) and the time-frequency (TF) polarization method (Burjánek *et al*., 2010; 2012) was achieved.

6.1. Results and discussion

A dense microtremor measurement survey was carried out focusing attention on the NE part of the bay, in which there is major evidence of slope instability and in which a high level of cliff fracturing is evident. Recording sites were located in order to sample the area as uniformly as possible. Moreover, several recording sites where chosen on a linear deployment for investigating the role of the fractures in the HVNR behaviour. The measurements were performed in three different zones: indeed, we carried out one set of recordings in a stable platform and far away from the cliff edge, a set of measurements in the fractured area along the cliff, and another set on the landslide body (see Fig. 18 for measurement points location). Examples of the spectral ratios obtained in the three different zones are shown in Figure 19a. The results allowed us to identify a region, away from the cliff edge, where the HVNR peaks are around a stable frequency of about 1.5 Hz. These fundamental peaks may be generally associated with the interface separating the BC layer from the underlying carbonates of the Globigerina Limestone formation (GL). Moreover, the presence of the BC layer gives rise to a velocity inversion since it has a lower shear wave velocity with respect to the overlying UCL formation. This causes the HVNR values to drop below 1 unit over a wide frequency range (Di Giacomo et al., 2005). The origin of the resonance peak as linked to the BC/GL interface was confirmed by the results obtained through a 1D modelling, performed by computing the synthetic HVNR curves (Fig. 19b). To compute the synthetic spectral ratios we considered that ambient vibrations wavefield can be represented by the superimposition of random multi modal plane waves moving in all the directions at the surface of a flat 1-D layered visco-elastic solid, as in Herrmann (2002) formulation, extending the modal summation up to the fifth mode. We also applied initial constraints on the thicknesses and elastic parameters of the layers using borehole logs data and we took shear waves velocity values from a separate preliminary study carried out in the same area using the ReMi, MASW and Refraction methods (Panzera *et al.*, 2011a). Similar behaviour to the above is observed in the spectral ratio obtained at sites close to the cliff edge and all around the identified fractures, but with slightly different features at the high-frequency interval. We observe indeed a clear and predominant peak at around 1.5 Hz, which is associated with the interface between BC and GL, and several smaller peaks at higher frequency (> 9.0 Hz). The fact that these peaks are not visible in the unfractured region leads us to postulate that they may be associated with the presence of fractures and of blocks almost detached from the cliff and therefore free to oscillate. Finally, the sites on the rock-fall area show a different HVNR behaviour with respect to the measurements taken on the plateau. In this area it is possible to identify HVNRs showing bimodal dominant peaks at low frequency, in the range 1.0-3.0 Hz, as well as pronounced peaks at about 3.0 Hz and at frequency higher than 9.0 Hz. The bimodal peaks at low frequency (1.0-3.0 Hz) can, in our opinion, be associated with the contact between the rockfall and detritus unit and the BC formation, as well as to the interface between BC and the underlying GL formation.

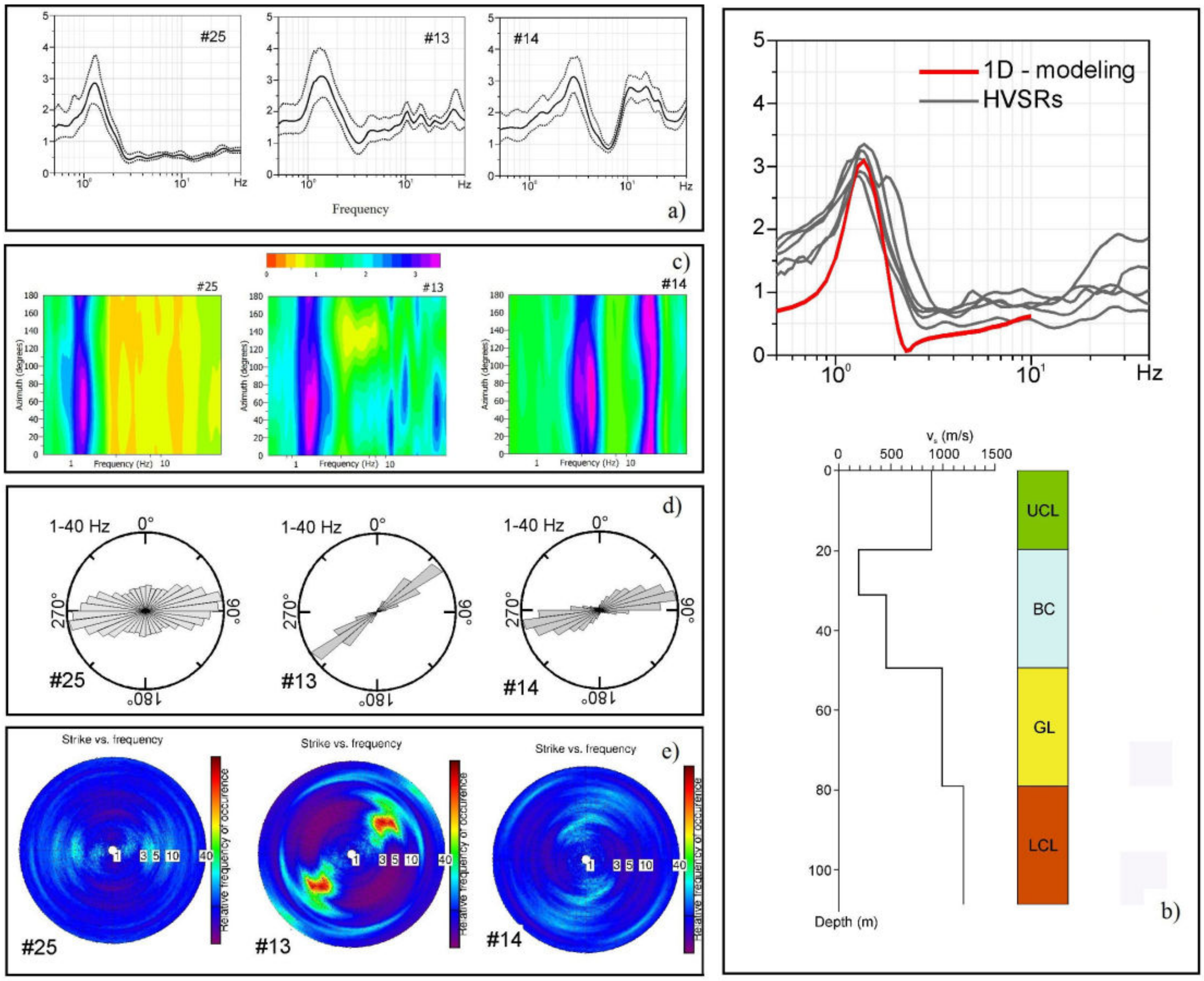

Figure 19. a) Example of HVNR results obtained at some recording sites located in the not fractured zone (#25), in the cliff area (#13), and in the landslide zone (#14); (b) results obtained through a 1D modelling, performed in sites located on the non-fractured zone, by computing the synthetic HVNR curve; (c) rotated HVNR, (d) rose diagrams and (e) polar plots obtained at recording sites #25, #13 and #14.

Inspection of directional effects (see examples in Fig. 19c) show that they are clearly evident in the cliff fracture zones,at an angle of about 40°-60° N in all the considered frequency range, although some variability in azimuth is observed at high frequency (>9 Hz) at site #13. On moving away from the cliff edge, the rotated HVNR show a slight change of the directional resonance angle and an amplitude decrease of the rotated spectral ratios at high frequency. Such a behavior could be linked to the increase of rock stiffness and a reduction of the blocks' freedom to oscillate. Finally, it is evident that the directionality pattern observed in the rotated HVSRs performed on the landslide body is quite complex. The general trend has a prevailing direction of about 40°-60° N at low frequency (1.0-9.0 Hz), similarly to what is observed in the fractured zone, whereas different resonant frequencies and directions that could be ascribed to the vibration of smaller blocks can be observed at higher frequencies (9.0-40.0 Hz). Furthermore, we obtained a direct estimate of the polarization angle through the full use of the three-component vector of the noise wave-field. General behavior of the noise wave-field, in this frequency range is shown through rose diagrams, whereas, in order to distinguish between properties of low and high frequency components of the signal, strike versus frequency polar plots were obtained. The examples shown in Figure 19d and e show that the maxima of the horizontal polarization occur in the north-east to east-north- east direction, although in some cases the high frequency directionality is more complex. As observed by Burjánek et al. (2010), high-frequency ground motion can indeed reflect the vibration of smaller blocks that imply both different resonant frequencies and directions. The polarization observed for the sites located away from the unstable areas (see e.g. #25 in Figure 19) show a trend with more dispersed and variable directions. The boundaries of the landslide area therefore appear well defined by the polarization pattern and as postulated by Kolesnikov et al. (2003) the landslide activity is characterized by strong horizontal polarization in a broad frequency band. In our study, a tendency seems evident for the entire landslide body to generally vibrate with a north-east azimuth and it may be assumed that, during a strong earthquake the ground motion would be amplified in this direction. Studies of Burjánek *et a*l. (2010; 2012) point out that the ambient noise polarization take place at about 90 degree angle to the observed fractures which are perpendicular to the sliding direction. In the present study the polarization angle is parallel to the opening cracks, which appears in contrast to the above mentioned results. A possible explanation of our findings is that there exists a prevailing north-easterly sliding direction of the landslide body which is strongly affecting the polarization direction especially in the 1-10 Hz frequency range.

In Figure 20 we summarize the above results into a tentative draft profile, located as shown in Fig. 18, which illustrates the main geological features and hypothesizes the shape of the landslide body. The bottom panel shows a 2-D diagram obtained by combining all the ambient noise measurements along the profile. Moving along the profile from measurement point #5 to #17, it is interesting to observe the increasing amplitude of the HVNR at frequencies greater than 6.0-7.0 Hz. It can also be noticed that, especially between 50 and 60 m along the profile (sites #1, #2 and #3) the influence of the fracture zone is evident (see dashed area in Fig. 20). This is associated with the vibrational mode of the almost detached blocks. Along the cross section, at distances ranging from 60 to 100 m, it is possible to note both the presence of the bimodal peak associated with the two interfaces detritus/BC and BC/GL, as well as the high frequency peaks most probably associated with the vibration of large blocks that have been detached from the cliff-face and are now partially or totally included in the BC.

As final considerations, it is noteworthy to observe that this study highlights the importance of evaluating the local seismic response in presence of slope instabilities related to landslide hazard. The instability processes that could be potentially triggered are linked to both slow mass movements, which might normally occur in tens or hundreds of years, and to sudden rockfall in the case of ground shaking due to moderate-to-strong earthquake activity. It is worth noting that:

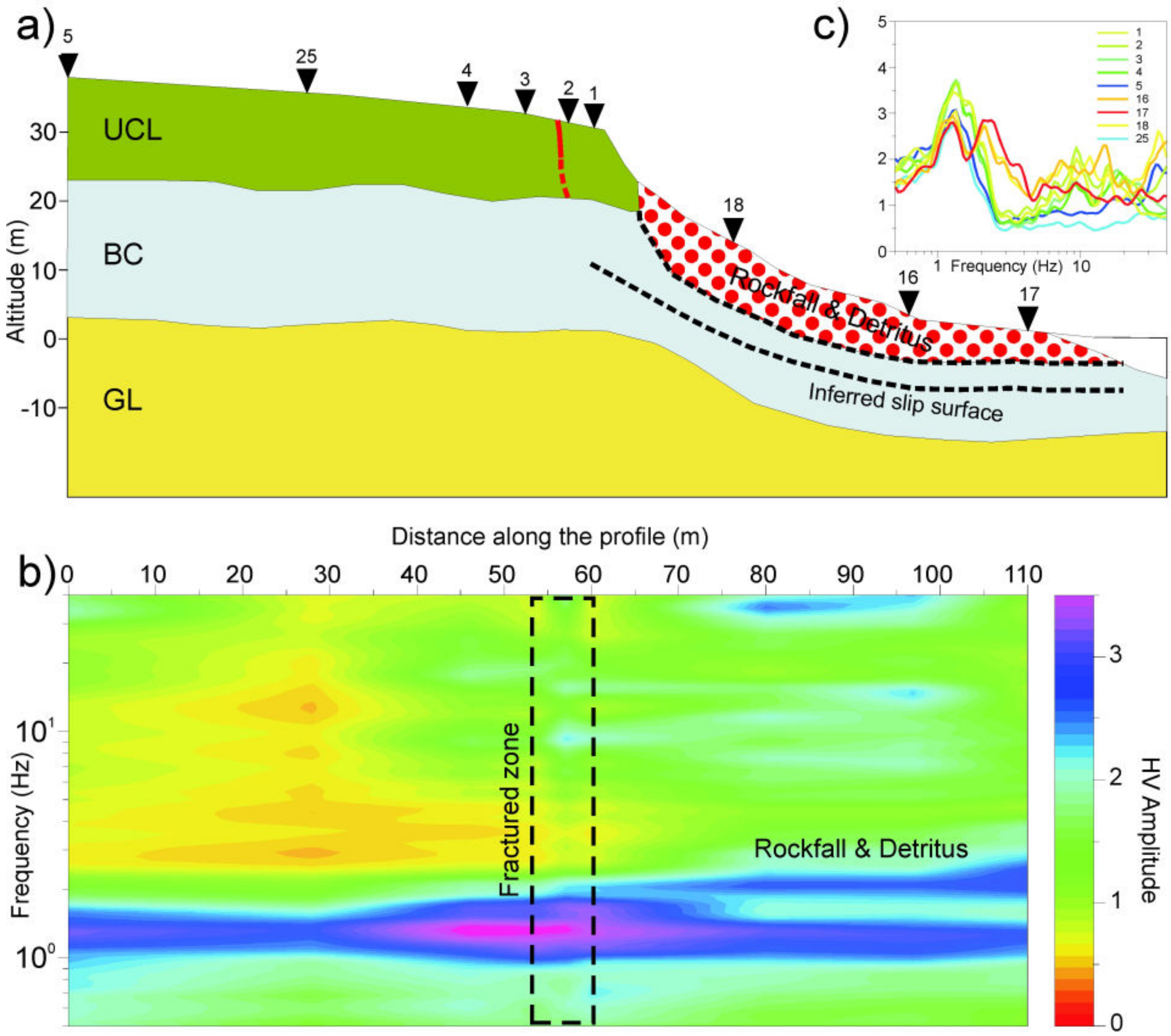

Figure 20. a) Cross section along the A-B profile in Fig. 27; b) 2-D diagram obtained combining all the ambient noise measurements along the profile as a function of distance (x axis) and frequency (y axis); c) HVSR results at the recording sites located across the profile.

- The use of noise measurements indicates that, at least in case of rockfall landslides, the existence of different zones characterized by differences in the dominant spectral ratio peaks that can be related to the presence of shallow lithotypes as well as to the existence of the fractures in the rock and active slip surface that allows the slow sliding of the upper landslide body.

- The instrumental observations indicate that the seismic ground motion can be considerably amplified and such amplification has a directional character that appear related with topographic, lithologic and structural features as well as normal mode rock slope vibration.

- The results of horizontal-to-vertical spectral ratio measurements indicate that this method could be useful for the recognition of site response directional phenomena.

http://dx.doi.org/10.5772/55439

7. Local site effects linked to the topography

The evaluation of the local seismic response when affected by the presence of topographic irregularities is particularly important, from the engineering point of view, mostly since a number of historical villages in Italy are erected on the top of natural reliefs. The influence of the topography on ground motion is linked to the sharpness of the ridge crest (Géli *et al*., 1988; Bard and Riepl-Thomas, 1999). Amplification effects are generally linked to the focalization of seismic waves at topmost part of a hill, due to the existence of diffraction, reflection, and conversion of the incident waves (Bard, 1982). They appear also frequency-dependent so that resonance phenomena occur when the wavelength of the incident wave is comparable to the horizontal dimension of the hill. In addition, significant directional effects, transverse to the major axis of the ridge, are often observed (Spudich *et al.*, 1996).

Several analytical and numerical methods have been developed to study incoming seismic waves when crossing a hill shaped morphology (*e.g.*, LeBrun *et al.*, 1999; Paolucci, 2002). Although experimental studies using earthquake instrumental records are relatively few, the use of earthquake data has shown to be a successful tool for the evaluation of topographic effects, as well as artificial explosions and ambient noise records, processed with the HVNR technique (*e.g.*, Borcherdt, 1970; LeBrun *et al.*, 1999; Poppeliers and Pavlis, 2002; Pagliaroli *et al.*, 2007).

The present study was performed in two reliefs having different morphologic and geologic features aiming to discriminate the topographic from the stratigraphic effects, using experimental techniques based on earthquake and ambient noise recordings in order to test at the same time the reliability of ambient noise recordings, processed through HVNR techniques, to estimate topographic effects. The first relief investigated is the area of Ortigia (downtown Siracusa, Sicily). It is a hill shaped peninsula, mostly formed by a carbonate sequence, elongated in the N-S direction, reaching a length of about 1,500 m, with a maximum height of 30 m a.s.l., having a transverse section width of about 700 m (Fig. 21). The second test area is the university campus (S. Sofia hill), a ridge located in the northern part of Catania (Fig. 22). The S. Sofia hill has a gentle topography with a flat surface at the top, it is elongated for about 700 m in NW-SE direction with a maximum height of 40 m. Its longitudinal section (B-B′ in Fig. 22) is asymmetric, consequently the northwestern side is quite gentle with respect to the southeastern part. On the other hand, the transverse section is more regular and symmetric (A-A′ in Fig. 22), with a base having width of about 500 m. This area has a more complex geology. The most frequently cropping out lithotype is basaltic lava that in pre-historical and historical times flowed onto the valleys originally existing in the sedimentary formations, formed by sand and gravel, laying over a marly clays basement.

In both areas several ambient noise measurements were performed, processing data with spectral ratio techniques and evaluating the directional effects as well. Moreover, in the S. Sofia area three permanent stations located respectively on the top of the hill, along the slope and at a reference site, about three kilometers away from the study area (see Fig. 22a, b). The area was monitored for about two years and a set of 44 local and regional seismic events, having a good signal-to-noise ratio was selected and processed using HVSR and SSR techniques.

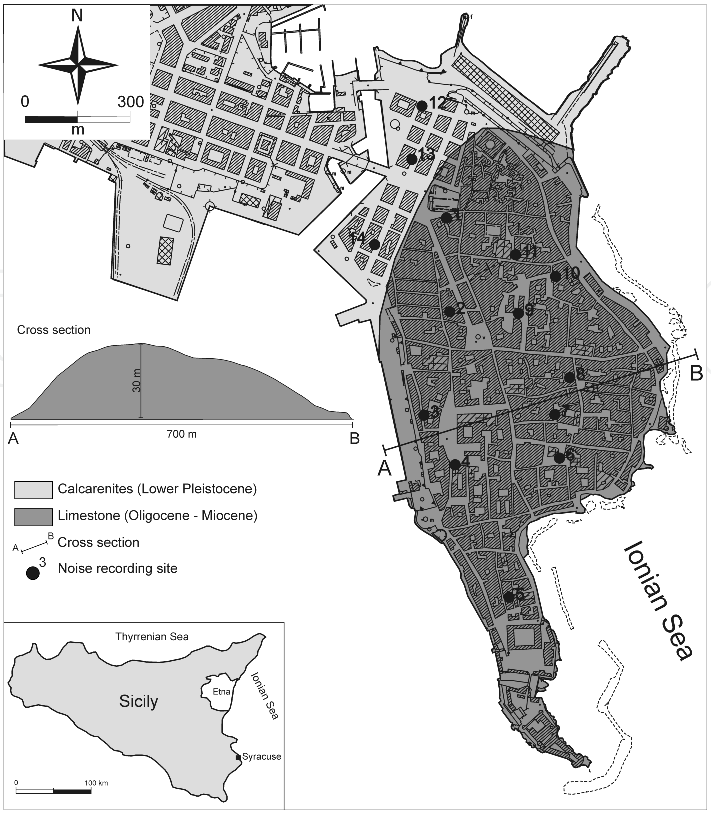

Figure 21. Geolithologic map of Ortigia (downtown Syracuse).

7.1. Results and discussion

Figure 23 shows a direct comparison of the rotated HVNRs, in the frequency band 1.0-10.0 Hz, and the results of noise polarization analysis for the same recording sites, filtering the signal in the range 1.0-3.0 Hz. Both methodologies agree, indicating, particularly in the frequency range 1.0–3.0 Hz, that maxima of HVNR amplitudes take place at 90–100° and maxima of the horizontal polarization strike in the E-W direction. We also compared field data observations with the theoretical resonance frequency (f_0) expected for the topographic effects in Ortigia hill. We adopted the relationship $f_0 = Vs/L$ (Bouchon, 1973; Géli *et al.*, 1988), where L is the width of the hill (about 700 m) and Vs is the shear wave velocity of the limestone outcropping in the peninsula (1,000 m/s). The predicted value, $f_0 = 1.4$ Hz, is consistent with the observed spectral ratio peaks, in the range of 1.0–3.0 Hz. In general, the amplification of ground motion connected to the surface topography is directly related to the sharpness of the topography (Bard, 1994). In such instances topographic effects become clearly detectable with experimental and numerical approaches. In our study, the gentle topography and the homogeneous lithology of the Ortigia peninsula make it an ideal and simple case study for investigating topographic effects using ambient noise records. The Ortigia hill has a natural frequency of about 1.4 Hz and shows an E-W preferential direction of vibration. The specific directional effects in ambient noise, well defined both in space and in a narrow frequency band (1.0–3.0 Hz), are signs of a normal mode of vibration of the hill (Roten *et al.*, 2006).

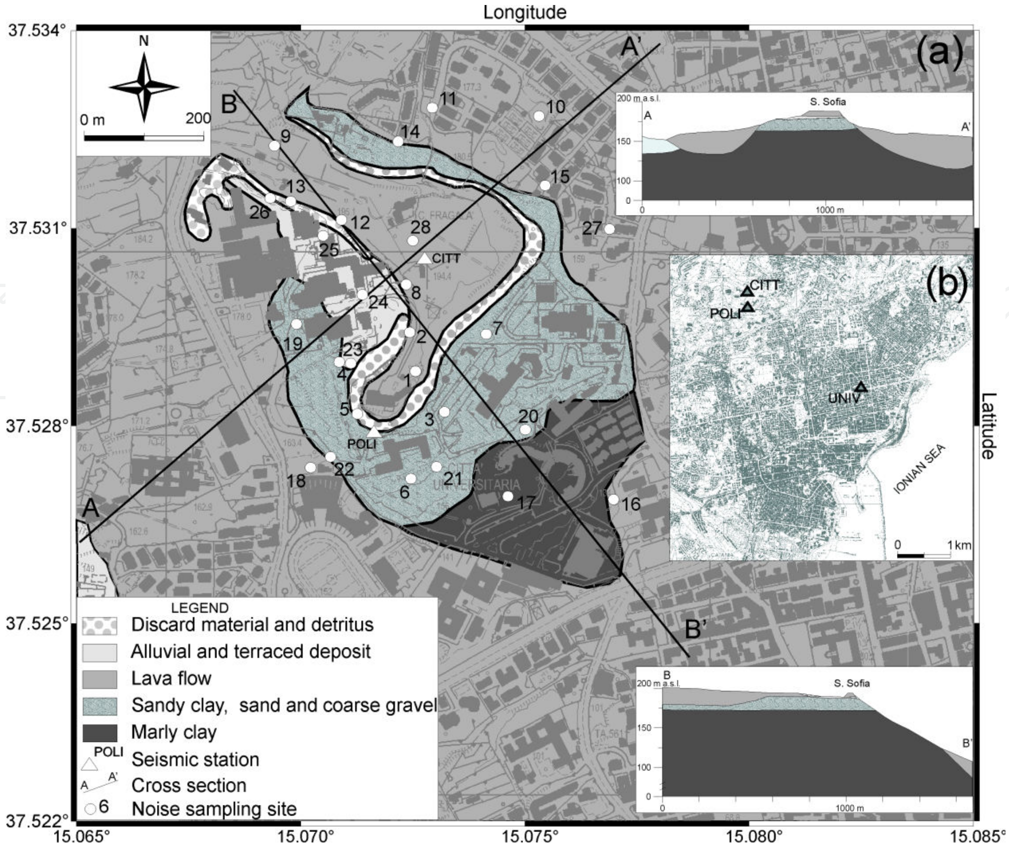

Figure 22. a) Geolithologic map of the S. Sofia hill; the insets show cross sections AA' and BB'. (b) location of the permanent stations with respect to the reference one (UNIV) (modified from Monaco et al., 2000).

The analysis performed in the other study case, (S. Sofia hill) indicate a more composite situation where both the complexity of surficial geology and the morphology significantly affect local amplification and directional effects. The results of SSR and HVSR are reported in Figure 24. Inspection of the Horizontal Standard Spectral ratio (HSSR) (Fig. 24a) point out that at the station CITT less pronounced spectral ratio peaks are observed with respect to the station POLI. The spectral ratio amplitudes obtained through the HVSR method appear underestimated in amplitude with respect to those obtained through the HSSR approach, however, especially at POLI, a good agreement between the two methodologies is observed as regards the frequency range of the dominant peaks (Fig. 24b). Moreover, it is interesting to observe that CITT and POLI stations show flat spectral ratio peaks, with HVSR amplitudes going down to values lower than 1 unit at frequencies higher than about 3.0 and 5.0 Hz, respectively. This appears related to the presence of a significant amplification of the vertical component of motion, as can be observed in the V/Vref plots (Fig. 24c). Such effect could be explained in terms of the complexity of the near-surface morphology and the existence of pronounced stratigraphic heterogeneities that, as postulated by many authors (e.g. Raptakis *et al.,* 2000; Bindi *et al.,* 2009), may affect the vertical component of motion. In any case, greater amplifications are observed in the HSSR at station POLI, in the frequency range 2.0-5.0 Hz and with smaller amplification values at CITT, in the range 1.0-2.0 Hz. This is different from what is usually expected for a topographic ridge, where major spectral ratio amplifications are

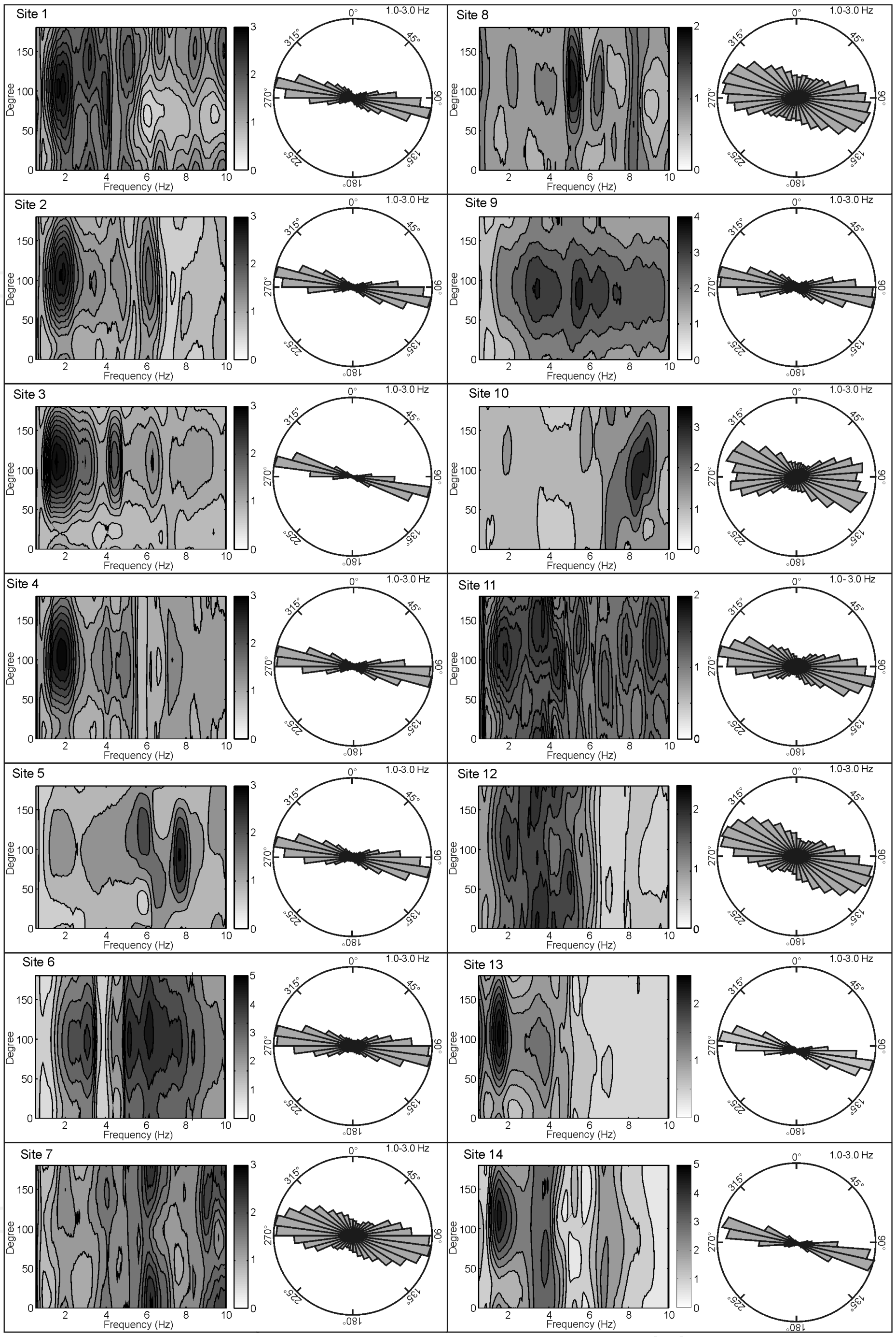

Figure 23. Contours of the geometric mean of the spectral ratios as a function of frequency (*x* axis) and direction of motion (*y* axis) and polarization rose diagrams calculated in the ranges 1–3 Hz.

supposed to take place at the top rather than along the slopes of the hill. This behavior, in our opinion, could be related to the gentle slope of the S. Sofia hill. In such conditions the reflection angle between the direction perpendicular to the free surface topography and the upward propagating wavefront is smaller than in the case of a steep slope. Therefore, the focusing effects at the crest are shadowed by laterally propagating waves (Boore, 1973) and it is reasonable to observe only moderate amplifications at the top of the hill. Moreover, it must be remembered that POLI is set on sedimentary terrains whereas CITT is located on a compact lava flow and such lithotype generally does not shows significant spectral ratio peaks as already observed by several authors (Lombardo and Rigano, 2007; Panzera et al, 2011b).

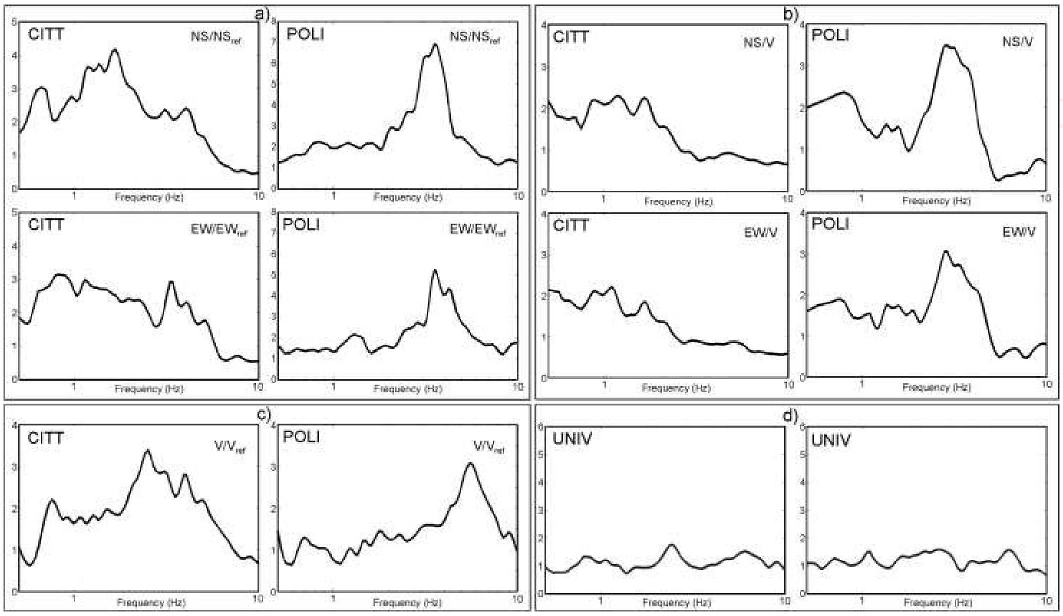

Figure 24. Spectral ratios (HSSR a), HVSR b) and VSSRc)) at permanent stations CITT and POLI; d) HVSR of the NS and EW components of motion at the reference site UNIV.

Ambient noise was recorded, in different lithotypes, along the slopes of the hill at decreasing height from the top (Fig. 22a), to identify possible topographical effects. The HVNRs show flat and, at times, deamplificated spectral ratios in several recording sites (see examples #9, #11, #16, #22 reported in Fig. 25) where the local geology consists in a sequence of thick (10-20 m) massive lava flows that overlie the sand and coarse gravel sediments lying on the marly clay basement. Conversely, when the sedimentary terrains outcrop (see examples #3, #4, #21, #23 reported in Fig. 25), significant spectral ratio peaks, are observed. Results obtained by the HVNR confirm the findings from earthquake data analysis and set into evidence that we are dealing with a geological setting more complex than a simple 1-D layered structure, for which the noise spectral ratio method was originally proposed. The presence of lava flows at the surface imply the existence of possible velocity inversions that give origin to H/V spectral amplitude lower than one unit (Castellaro and Mulargia, 2009; Di Giacomo *et al.*, 2005) and the existence of amplification in the vertical component of the ground motion.

The existence of directional amplification was investigated using both earthquake and ambient noise data. Directional analysis and polarization of the horizontal components of motion show less pronounced directional effect at CITT with respect to POLI station, where clear polarization effects at about 40° appear. The results of polarization analysis are depicted in Figure 26. The hodograms obtained from noise measurements show that the polarization azimuths are similar to those obtained by processing the earthquake data. It appears indeed confirmed that at the top of the studied hill (#9, #12, #14 and #28) the pattern of polarization directions is similar

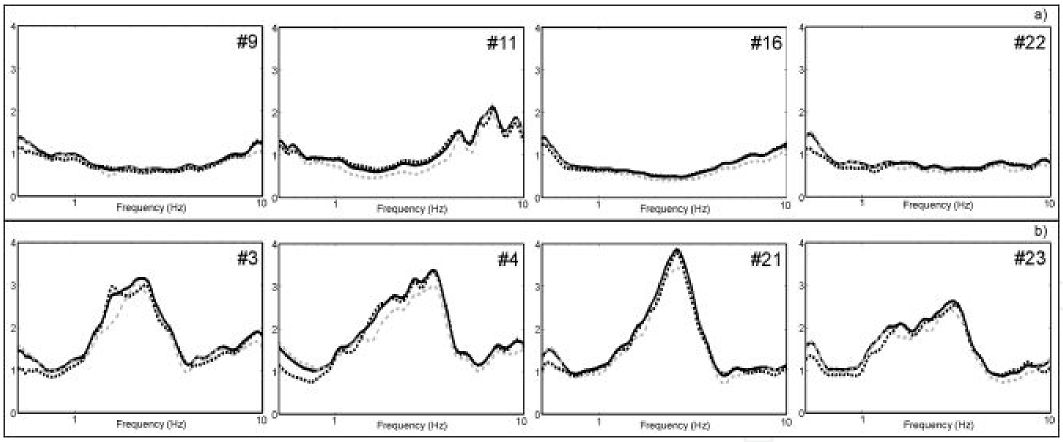

Figure 25. Examples of HVNR results at representative recording sites located on lava flows (a) and on sedimentary terrains (b); solid black lines refer to the average H/V spectra, dotted grey and black lines refers to NS/V and EW/V spectra, respectively.

to what is observed at the station CITT. On the other hand, the noise rose diagrams obtained at the other recording sites point out polarization azimuths that seem to be in agreement with the slope directions of the hill flanks. Only few sites (#17, #21, #22, #25) make an exception to such trend, showing a directional variability that could be linked to the local shallow lithologic features. The investigation on the characteristics of the site response at the S. Sofia hill, therefore set into evidence that the complexity of the near-surface geology, as well as the morphology strongly influence the local amplification of the ground motion and the directional effects. Findings of the present study confirm that major amplification effects do indeed take place on the sedimentary terrains which outcrop along the flanks of the hill. On the contrary, on the lava flows, a significant amplification of the vertical component of motion, is observed as a consequence of velocity inversion effects.

The results coming out from investigations performed in the two test areas allow us to draw the following general considerations about topographic effects:

- Ambient noise is a useful tool that can be widely adopted in site response evaluation and in studies of topographic irregularities as well, especially when a simplified topography and lithology is present. However, in the presence of lateral and vertical heterogeneities, as well as velocity inversions, a combined use of noise, earthquake data and theoretical models is advisable to correctly predict the site response behavior. In such instances topographic effects are more composite and a complex wavefield is observed.

- The wedge angle of the hill appears to play an important role since a wide angle reduces the focusing effects at the crest in favor of laterally propagating waves.

- Both the directional resonance and the polarization analysis confirm the presence of a directional effect transverse to the major axis of the ridge. This behavior is particularly evident in reliefs having a homogeneous simple convex morphology. In such instance the ridge oscillation can be considered similar to what is observed in civil structures, providing there is not significant soil-structure interaction and considering the building as a single-

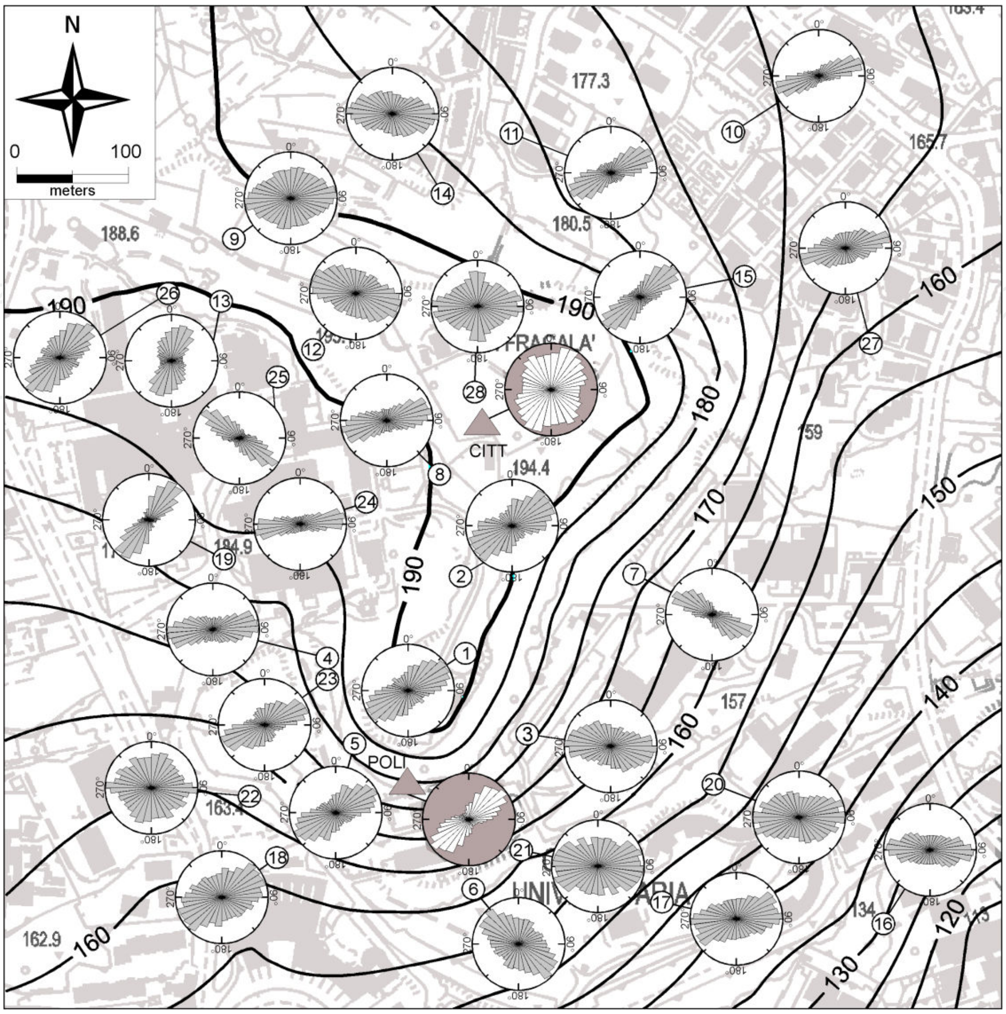

Figure 26. Ground motion polarization from noise measurements in the S. Sofia hill area; hodograms with a grey background refers to results coming from the analysis of earthquakes recorded at CITT and POLI stations.

degree-of-freedom damped oscillator (Gallipoli *et al*.2009). In such instances the vertical component of motion travels through the building without amplification, whereas the horizontal components undergo a significant amplification.

- As a practical implication of the present study it can be observed that the topographic effects cannot be easily evaluated especially when subsurface morphology and lithologic features are predominant.

8. Concluding remarks

The present study has tested the use of ambient noise recordings as a speedy technique for evaluating the local seismic response in several instances where either lithologic and/or morphologic and structural features can significantly affect the response of shallow geologic formations to a seismic input. Our findings further support the reliability of the use of ambient noise recordings for preliminary characterization of dynamic properties of terrains. Its employment has, in recent years, been widely used for site amplification studies since data acquisition time and costs are significantly reduced. Moreover, the HVNR technique can be largely adopted since it requires only one mobile seismic station with no additional measurements at rock sites for comparison. The ratio between the horizontal and vertical spectral components of motion can indeed reveal the fundamental resonance frequency of the site. It also does not require the long and simultaneous deployment of several instruments to collect a useful set of earthquake data.

Our results show also the importance of performing analysis to evaluate directional effects and polarization of the horizontal components of the ground motion. It has indeed to be remembered that directional effects cannot be neglected for a correct planning of edifices and man-made structures in order to reduce the potential risk of building damage as a result of ground motions.

Author details

F. Panzera[1], G. Lombardo[1], S. D'Amico[2*] and P. Galea[2]

*Address all correspondence to: sebdamico@gmail.com

1 Dipartiemnto di Scienze Biologiche, Geologiche ed Ambientali, Universita' di Catania, Italy

2 Department of Physics, University of Malta, Malta

References

[1] Acocella, V, & Neri, M. (2005). Structural features of an active strike-slip fault on the sliding flank of Mt. Etna (Italy). *J. Struct. Geol*, , 27, 343-355.

[2] Azzaro, R. (1999). Earthquake surface faulting at Mount Etna volcano (Sicily) and implications for active tectonics, *J. Geodyn.*, doi:10.1016/S0264-3707(98)00037-4., 28, 193-213.

[3] Azzaro, R, Branca, S, Gwinner, K, & Coltelli, M. (2012). The volcano-tectonic map of Etna volcano, 1:100.000 scale: an integrated approach based on a morphotectonic analysis from high-resolution DEM constrained by geologic, active faulting and seismotectonic data, Ital. J. Geosci., 131(1), 153-170, doi:IJG.2011.29.

[4] Azzaro, R, Mattia, M, & Puglisi, G. (2001). Dynamics of fault creep and kinematics of the eastern segment of the Pernicana fault (Mt. Etna, Sicily) derived from geodetic observations and their tectonic significance. *Tectonophysics*, 333(3-4), 401-415.

[5] Baratta, M. (1910). La catastrofe sismica Calabro-Messinese (28 dicembre 1908), *Società Geografica Italiana, Rom, 458 p*.

[6] Bard, P. Y. (1994). Effects of surface geology on ground motion: recent results and remaining issues. In: *G. Duma (ed), Proc. 10th European Conference on Earthquake Engineering. Wien, 28 Aug.-2 Sept., Balkema, Rotterdam*, , 1, 305-323.

[7] Bard, P. Y. (1999). Microtremor measurements: a tool for site effect estimation? In: *Irikura et al. (ed.), The effects of surface geology on seismic motion. Balkema, Rotterdam*, , 1251-1279.

[8] Bard, P. Y, & Riepl-thomas, J. (1999). Wave propagation in complex geological structures and their effects on strong ground motion. In *Wave motion in Earthquake Engineering*: edited by Kausel and Manolis, WIT Press, , 2, 37-95.

[9] Bardet, J. P, Ichii, K, & Lin, C. H. (2000). EERA, a computer program for Equivalent-linear Earthquake site Response Analyses of layered soil deposits. *University of Southern California, Department of Civil Engineering, user's manual*, 38p.

[10] Ben-zion, Y, Peng, Z, Okaya, D, Seeber, L, Armbruster, J. G, Ozer, N, Michael, A. J, Baris, S, & Aktar, M. (2003). A shallow fault-zone structure illuminated by trapped waves in the Karadere-Duzce branch of the North Anatolian Fault, western Turkey. *Geophys. J. Int*., , 152, 1-19.

[11] Ben-zion, Y, & Sammis, C. G. (2003). Characterization of fault zones, Pure Appl. Geophys., , 160, 677-715.

[12] Ben-zion, Y, & Sammis, C. G. (2009). Mechanics, Structure and Evolution of Fault Zones, Pure appl. Geophys.,*166*doi:10.1007/s00024-009-0509-y., 1533-1536.

[13] Bindi, D, Parolai, S, & Cara, F. Di Giulio G., Ferretti G., Luzi L., Monachesi G., Pacor F., Rovelli A. ((2009). Site amplifications observed in the Gubbio Basin, Central Italy: Hints for lateral propagation effects. *Bull. Seism. Soc. Am.*, 99(2A), , 741-760.

[14] Boore, D. M. (1973). The effect of simple topography on seismic waves: implications for the accelerations recorded at Pacoima Dam, San Fernando valley, California. *Bull. Seism. Soc. Am.*, 63(5), 1603-1609.

[15] Boore, D. M, Graizer, V. M, Tinsley, J. C, & Shaka, A. F. (2004). A study of possible ground-motion amplification at the Coyote Lake dam, California. *Bull. Seism. Soc. Am.*, doi:l., 94(4), 1327-1342.

[16] Borcherdt, R. D. (1970). Effects of local geology on ground motion near San Francisco Bay. *Bull. Seism. Soc. Am.*, , 60, 29-61.

[17] Bouchon, M. (1973). Effect of topography on surface motion. *Bull. Seism. Soc. Am.*, , 63, 615-632.

[18] Burjánek, J, Gassner-stamm, G, Poggi, V, Moore, J. R, & Fäh, D. (2010). Ambient vibration analysis of an unstable mountain slop. *Geophys. J. Int*., 180(2), 820-828. doi:j.X. 2009.04451.x, 1365-246.

[19] Burjánek, J, Moore, J. R, Molina, F. X. Y, & Fäh, D. (2012). Instrumental evidence of normal mode rock slope vibration. *Geophys. J. Int*., 188(2), 559-569.

[20] Calderoni, G, & Rovelli, A. Di Giovambattista R. ((2010). Large amplitude variations recorded by an on-fault seismological station during the L'Aquila earthquakes: evidence for a complex fault induced site effect. *Geophys. Res. Lett*., 37, L24305, doi: 10.1029/2010GL045697.

[21] Cara, F. Di Giulio G., and Rovelli A. ((2003). A study on seismic noise variations at Colfiorito, Central Italy: implications for the use of H/V spectral ratios. *Geophysical Research Letters* , 30(18), 1972-1976.

[22] Carbone, S, Branca, S, Lentini, F, Barbano, M. S, & Corsaro, M. A. Di Stefano A., Ferrara V., Monaco C., Longhitano S., Platania I., Zanini A., De Beni E. e Ferlito C. ((2009). Note Illustrative della Carta Geologica d'Italia alla scala 1:50000, foglio 634 Catania. *ISPRA, Servizio Geologico d'Italia, Organo Cartografico dello Stato, S.EL.CA. s.r.l., Firenze*.

[23] Castellaro, S, & Mulargia, F. (2009). The Effect of Velocity Inversions on H/V, *Pure appl. Geophys*. dois00024-009-0474-5., 166, 567-592.

[24] Catchings, R. D, & Lee, W. H. K. (1996). Shallow velocity structure and Poisson's ratio at the Tarzana, California, strong-motion accelerometer site. *Bull. Seism. Soc. Am., 86*, 1704-1713.

[25] Chavez-garcia, F. J, Sanchez, L. R, & Hatzfeld, D. (1996). Topographic site effects and HVSR. A comparison between observations and theory. *Bull. Seism. Soc. Am.*, , 86, 1559-1573.

[26] Cultrera, G, Rovelli, A, Mele, G, Azzara, R, Caserta, A, & Marra, F. (2003). Azimuth-dependent amplification of weak and strong ground motions within a fault zone (Nocera Umbra, central Italy). *J. Geophys. Res., 108* (B3), 2156 doi:JB001929.

[27] Del Gaudio VCoccia S., Wasowski J., Gallipoli M. R., Mucciarelli M. ((2008). Detection of directivity in seismic site response from microtremor spectral analysis. *Natural Hazards and Earthquake System Science* , 8, 751-762.

[28] Del Gaudio VWasowski J. ((2011). Advances and problems in understanding the seismic response of potentially unstable slopes. *Engineering geology*, 122, 1-2, 73-83.

[29] Di Giacomo DGallipoli M.R., Mucciarelli M., Parolai S., Richwalski S.M. ((2005). Analysis and modeling of HVSR in the presence of a velocity inversion: the case of Venosa, Italy. *Bull. Seism. Soc. Am.* , 95, 2364-2372.

[30] Di Giulio GCara F., Rovelli A., Lombardo G., Rigano R. ((2009). Evidences for strong directional resonances in intensely deformed zones of the Pernicana fault, Mount Etna, Italy. *J. Geophys. Res.*, 114, B10308, doi:10.1029/2009JB006393.

[31] Di Grazia GFalsaperla S., Langer H. ((2006). Volcanic tremor location during the 2004 Mount Etna lava effusion. *Geophys. Res. Lett.*, 33, L04304, doi:10.1029/2005GL025177.

[32] Gallipoli, M. R, Mucciarelli, M, & Vona, M. (2009). Empirical estimate of fundamental frequencies and damping for Italian buildings. *Earthquake Engineering and Structural Dynamics* doi:eqe.878.

[33] Geli, L, Bard, P. Y, & Jullien, B. (1988). The effect of topography on earthquake ground motion: a review and new results. *Bull. Seism. Soc. Am.*, , 78, 42-63.

[34] Grasso, M, & Lentini, F. (1982). Sedimentary and tectonic evolution of the eastern hyblean plateau (South-Eastern Sicily) during Late Cretaceous to Quaternary time. *Paleoecology* , 39, 261-280.

[35] Herrmann, R. B. (2002). Computer programs in seismology. St. Louis University,, 4

[36] Hudson, M, Idriss, I. M, & Beikae, M. a computer program to evaluate the seismic response of soil structures using finite element procedures and incorporating a compliant base. *Center for Geotechnical Modeling, Department of Civil and Environmental Engineering*, University of California Davis, Davis California.

[37] Ibs-Von Seth MWohlenberg J. ((1999). Microtremor measurements used to map thickness of soft sediments. *Bull. Seism. Soc. Am.*, , 89, 250-259.

[38] Igel, H, Jahnke, G, & Ben-zion, Y. (2002). Numerical simulation of fault zone trapped waves: Accuracy and 3-D effects. *Pure Appl. Geophys.*, , 159, 2067-2083.

[39] Illies, J. H. (1981). Graben formation: the Maltese Islands, a case history, Tectonophysics, , 73, 151-168.

[40] Irikura, K, & Kawanaka, T. (1980). Characteristics of microtremors on ground with discontinuous underground structure. *Bull. Disaster Prev. Inst. Kyoto Univ.*, 30(3), 81-96.

[41] Jurkevics, A. (1988). Polarization analysis of three component array data, *Bull. Seism. Soc. Am.*, , 78, 1725-1743.

[42] Kolesnikov, Y. I, Nemirovich-danchenko, M. M, Goldin, S. V, & Seleznev, V. S. (2003). Slope stability monitoring from microseismic field using polarization methodology. *Natural Hazards and Earth System Sciences*, , 3, 515-521.

[43] Kramer, S. L. (1996). Geotechnical Earthquake Engineering. Prentice Hall, New Jersey.

[44] Lachet, C, & Bard, P. Y. (1994). Numerical and theoretical investigations on the possibilities and limitations of Nakamura's techniques. *Journal of Physics of the Earth* , 302(42), 377-397.

[45] LeBrun BHatzfeld D., Bard P.Y., Bouchon M. ((1999). Experimental study of the ground motion on a large scale topographic hill at Kitherion (Greece). *Journal of Seismology* , 3, 1-15.

[46] Lee, M. K. W, & Finn, W. D. L. (1978). DESDRA-2 Dynamic effective stress response analysis of soil deposits with energy transmitting boundary including assessment of liquefaction potential. *Soil Mechanics Series n. 38,* University of British Colombia, Vancouver.

[47] Lentini, F, Carbone, S, & Guarnieri, P. (2006). Collisional and postcollisional tectonics of the Apenninic-Maghrebian orogen (southern Italy). In: Dilek Y. & Pavlides S. (eds.), «Postcollisional tectonics and magmatism in the Mediterranean region and Asia». GSA Special Paper, , 409, 57-81.

[48] Lermo, J, & Chavez-garcia, F. J. (1993). Site effect evaluation using spectral ratio with only one station. *Bull. Seism. Soc. Am.*, , 83, 1574-1594.

[49] Lewis, M. A, Peng, Z, Ben-zion, Y, & Vernon, F. L. (2005). Shallow seismic trapping structure in the San Jacinto fault zone near Anza, California. *Geophys. J. Int.*, , 162, 867-881.

[50] Li, Y. G, Aki, K, Adams, D, & Hasemi, A. (1994). Seismic guided waves in the fault zone of the Landers, California, earthquake of 1992. *J. Geophys. Res.*, , 99, 11705-11722.

[51] Li, Y. G, Vidale, J. E, Aki, K, & Xu, F. (2000). Depth-dependent structure of the Landers fault zone using fault zone trapped waves generated by aftershocks. *J. Geophys. Res.*, , 105, 6237-6254.

[52] Lombardo, G, & Rigano, R. (2006). Amplification of ground motion in fault and fracture zones: observations from the Tremestieri fault, Mt. Etna (Italy). *J. Volcanol. Geotherm. Res.*,, 153, 167-176.

[53] Lombardo, G, & Rigano, R. (2007). Local seismic response in Catania (Italy): A test area in the northern part of the town. *Engineering Geology* , 94, 38-49.

[54] Lombardo, G, & Rigano, R. (2010). Local seismic response evaluation in natural and artificial cavities. *Proceedings 3rd International Symposium "Karst Evolution in the South Mediterranean Area", 29-31 May 2009, Ragusa, Italy*, Speleologia Iblea C.I.R.S. ISNN 1123-9875., 14

[55] Mantovani, M, Devoto, S, Forte, E, Mocnik, A, Pasuto, A, Piacentini, D, & Soldati, M. (2012). A multidisciplinary approach for rock spreading and block sliding investigation in the north-western coast of Malta. *Landslides*, DOIs10346-012-0347-3

[56] MEPA (Malta Environment and Planning AuthorityMapping Unit) ((2004). Xemxjia bay area map 1:2500.

[57] Mizuno, T, & Nishigami, K. (2006). Deep structure of the Nojima fault, southwest Japan, estimated from borehole observation of fault-zone trapped waves. *Tectonophysics*, , 417, 231-247.

[58] Mcguire, W. J, & Pullen, A. D. (1989). Location and orientation of eruptive fissures and feeder-dykes at Mount Etna: influence of gravitational and regional stress regimes. *J. Volcanol. Geotherm. Res.* , 38, 325-344.

[59] Monaco, C, Catalano, S, De Guidi, G, Gresta, S, Langer, H, & Tortorici, L. (2000). The geological map of the urban area of Catania (Eastern Sicily): morphotectonic and seismotectonic implications. *Mem. Soc. Geol. It.*, , 55, 425-438.

[60] Monaco, C, Tapponnier, P, Tortorici, L, & Gillot, P. Y. (1997). Late Quaternary slip rates on the Acireale-Piedimonte normal faults and tectonic origin of Mt. Etna (Sicily). *Earth Planet. Sci. Letters*, , 147, 125-139.

[61] Nakamura, Y. (1989). A method for dynamic characteristics estimation of subsurface using microtremor on the ground surface. *Q.R. Railway Tech. Res. Inst. Rept.*, , 30, 25-33.

[62] Neri, M, Acocella, V, & Behncke, B. (2004). The role of the Pernicana Fault System in the spreading of Mt. Etna (Italy) during the 2002-2002 eruption. *Bullettin of Volcanology* doi:10.1007/S00445-003-0322-X., 66, 417-430.

[63] Neri, M, Guglielmino, F, & Rust, D. (2007). Flank instability on Mount Etna: Radon, radar interferometry, and geodetic data from the southwestern boundary of the unstable sector, *J. Geophys. Res.*, 112, B04410, doi:10.1029/2006JB0047

[64] Nogoshi, M, & Igarashi, T. (1970). On the propagation characteristics of microtremors. *Journal of the Seismological Society of Japan* , 23, 264-280.

[65] Nunziata, C, Natale, M, & Panza, G. F. (1999). b. Estimation of cavity effects on response spectra for the 1980 earthquake in the historical centre of Naples. In: *Earthquake Geotechnical Engineering,* Sêco & Pinto (Eds), Balkema, Rotterdam, , 9-14.

[66] Pagliaroli, A, Pitilakis, K, Chávez-garcía, F. J, Raptakis, D, Apostolidis, P, Ktenidou, O. J, Manakou, M, & Lanzo, G. (2007). Experimental study of topographic effects using explosions and microtremors recordings, paper presented at 4th International Conference on Earthquake Geotechnical Engineering, Thessaloniki, Greece.

[67] Paolucci, R. (2002). Amplification of earthquake ground motion by steep topographic irregularities. *Earthquake Engineering and Structural Dynamics 31*, 1831-1853.

[68] Panzera, F, Pace, S, D'Amico, , Galea, S, & Lombardo, P. G. ((2011a). Preliminary results on the seismic properties of main lithotypes outcropping on Malta. *GNGTS 30° Convegno Nazionale, Mosetti tecniche grafiche, Trieste*, , 306-308.

[69] Panzera, F, Rigano, R, Lombardo, G, & Cara, F. Di Giulio G., Rovelli A. ((2011b). The role of alternating outcrops of sediments and basaltic lavas on seismic urban scenario: the study case of Catania, Italy. *Bulletin of Earthquake Engineering* dois10518-010-9202-x., 9, 411-439.

[70] Pedley, H. M, Clark, M, & Galea, P. (2002). Limestone isles in a cristal sea: the geology of the Maltese islands. *P.E.G. Ltd*, 9-99090-318-2

[71] Pedley, H. M, House, M. R, & Waugh, B. (1978). The geology of the Pelagian block: the Maltese Islands. In: *Narin, A. E. M., Kanes, W. H., and Stehli, F. G. (eds), The Ocean Basin and Margins, 4B: The Western Mediterranean, Plenum Press*, London, , 417-433.

[72] Peng, Z, & Ben-zion, Y. (2006). Temporal changes of shallow seismic velocity around the Karadere-Duzce Branch of the North Anatolian Fault and strong ground motion. *Pure Appl. Geophys*. , 163, 567-600.

[73] Pischiutta, M, Salvini, F, Fletcher, J, Rovelli, A, & Ben-zion, Y. (2012). Horizontal polarization of ground motion in the Hayward fault zone at Fremont, California: dominant fault-high-angle polarization and fault-induced cracks. *Geophys. J. Int*. 188(3), 1255-1272.

[74] Pitilakis, K. (2004). Chapter 5: Site Effects. In: *Recent advances in Earthquake Geothecnical Enginnering and Microzonation,* A. Ansal ed., Kluwer Academic Publishers, , 139-198.

[75] Poppeliers, C, & Pavlis, G. L. (2002). The seismic response of a steep slope: high-resolution observations with a dense, three-component seismic array. *Bulletin of the Seismological Society of America 92*(8), 3102-3115.

[76] Raptakis, D, Chavez-garcia, F. J, Makra, K, & Pitilakis, K. (2000). Site effects at Euroseistest- I. Determination of the valley structure and confrontation of observations with 1D analysis. *Soil Dynamics and Earthquake Engineering* , 19, 1-22.

[77] Reuther, C, & Eisbacher, D. a. n. d G. H. (1985). Pantelleria Rift- crustal extension in a convergent intraplate setting. Geol. Rndsch., , 74, 585-597.

[78] Riedel, W. (1929). Zur Mechanik Geologischer Brucherscheinungen. Zentral-blatt fur Mineralogie, Geologie und Paleontologie B, , 354-368.

[79] Rigano, R, Cara, F, Lombardo, G, & Rovelli, A. (2008). Evidence of ground motion polarization on fault zones of Mount Etna volcano. *J. Geophys. Res*.,113, B10306, doi: 10.1029/2007JB005574.

[80] Rigano, R, & Lombardo, G. (2005). Effects of lithological features and tectonic structures in the evaluation of local seismic response: an example from Hyblean plateau (Eastern Sicily). *Geologica Carpathica, 564297306*

[81] Roten, D, Cornou, C, Fäh, D, & Giardini, D. (2006). D resonances in Alpine valleys identified from ambient vibtation wavefields. *Geophysical Journal International* , 165, 889-905.

[82] Rovelli, A, Caserta, A, Marra, F, & Ruggiero, V. (2002). Can seismic waves be trapped inside an inactive fault zone? The case study of Nocera Umbra, central Italy. *Bull. Seismol. Soc. Am.*, , 92, 2217-2232.

[83] Rust, D, & Neri, M. (1996). The boundaries of large-scale collapse on the flanks of Mount Etna, Sicily, In: *Volcano Instability on the Earth and Other Planets, edited by W.M. McGuire, A.P. Jones and J. Neuberg*, Spec. Pub. Geol. Soc. London, , 110, 193-208.

[84] Scherbaum, F, Hinzen, K. G, & Ohrnberger, M. (2003). Determination of shallow shear wave velocity profiles in the Cologne, Germany area using ambient vibrations. *Geophys. J. Int.*, , 152, 597-612.

[85] Schnabel, B, Lysmer, J, & Seed, H. (1972). SHAKE: a computer program for earthquake response analysis of horizontally layered sites. *Rep. E.E.R.C. 7212Earthq. Eng. Research Center,* Univ. Califormia, Berkeley.

[86] SESAME ((2004). Guidelines for the implementation of the H/V spectral ratio technique on ambient vibrations: Measurements, processing and interpretation. SESAME European Research Project WP12, deliverable D23.12, http://sesame-fp5.obs.ujf-grenoble.fr/Deliverables.

[87] Seeber, L, Armbruster, J. G, Ozer, N, Aktar, M, Baris, S, Okaya, D, Ben-zion, Y, & Field, E. (2000). The 1999 Earthquake Sequence along the North Anatolia Transform at the Juncture between the Two Main Ruptures, In: *The 1999 Izmit & Duzce Earthquakes: preliminary results, edit. Barka A., O. Kazaci, S. Akyuz & E. Altunel*, Istanbul technical university, , 209-223.

[88] Sgarlato, G, Lombardo, G, & Rigano, R. (2011). Evaluation of seismic site response nearby underground cavities using earthquake and ambient noise recordings: a case study in Catania area, Italy. *Engineering Geology*. doij.enggeo.2011.06.002., 122, 281-291.

[89] Spudich, P, Hellweg, M, & Lee, W. H. K. (1996). Directional topographic site response at Tarzana observed in aftershocks of the 1994 Northridge, California, earthquake: implications for mainshock motions. *Bull. Seism. Soc. Am.*, 86(1B), SS208., 193.

[90] Tchalenko, J. S. (1968). The evolution of kink-bands and the development of compression textures in sheared clays, Tectonophysics, , 6, 159-174.

[91] Various Authors(1993). Geological Map of the Maltese Island. Sheet Malta- Scale 1:25,000. Oil Exploration Directorate, Office of the Prime Minister, Malta,., 1.

[92] Wood, H. O. (1908). Distribution of apparent intensity in San Francisco, in the California earthquake of April 18, 1906. *Report of the State Earthquake Investigation Commission, Canergie Institute of Washington, Washington, D.C.,* , 1